NASA CONTRACTOR REPORT

NASA CR-272

A STUDY OF TWO PHASE DETONATION AS IT RELATES TO ROCKET MOTOR COMBUSTION INSTABILITY

by J. A. Nicholls, E. K. Dabora, and K. W. Ragland

Prepared under Contract No. NASr-54(07) *by*
UNIVERSITY OF MICHIGAN
Ann Arbor, Mich.
for

NATIONAL AERONAUTICS AND SPACE ADMINISTRATION • WASHINGTON, D. C. • AUGUST 1965

NASA CR-272

A STUDY OF TWO PHASE DETONATION AS IT RELATES TO ROCKET MOTOR COMBUSTION INSTABILITY

By J. A. Nicholls, E. K. Dabora, and K. W. Ragland

Prepared under Contract No. NASr-54(07) by
UNIVERSITY OF MICHIGAN
Ann Arbor, Mich.

for

NATIONAL AERONAUTICS AND SPACE ADMINISTRATION

For sale by the Clearinghouse for Federal Scientific and Technical Information
Springfield, Virginia 22151 – Price $4.00

ACKNOWLEDGMENT

The authors wish to acknowledge the active participation of G. R. Olsson, Assistant Research Engineer, who contributed the section on the theoretical aspects of two phase detonations and of A. A. Ranger, Assistant Research Engineer, and S. A. Crist, Assistant in Research, who are responsible for the design and operation of the shock tube for the drop shattering experiments. The authors are also thankful to R. E. Cullen, Research Engineer, for his general advice throughout this study and to C. J. Iott, Technician, for his help in obtaining the photographs on spray detonations.

TABLE OF CONTENTS

ABSTRACT

A simplified treatment of the jump conditions in two phase detonations that takes into account a change in the molecular weight and the ratio of the specific heats is made. It shows significant differences between these jump conditions and their all-gaseous counterparts. The experimental setup for studying two phase detonations is described. Detonation or "detonation-like" waves propagating at 5300-5700 ft/sec are observed in diethylcyclohexane sprays in gaseous oxygen. A pressure ratio of the order 30 which is too high for a Chapman-Jouguet wave but compatible with its associated shock wave is observed. The speed of the wave is lower than what is expected theoretically, apparently because of incomplete combustion. Detonation waves at even lower velocities are also observed when the walls of the detonation tube are wetted by the fuel. This observation is considered significant to rocket motor instability.

Means of producing monodisperse sprays which would be adaptable to this study are discussed. They are based on the instability of capillary jets when mechanically disturbed. It is expected that a field of uniform-size drops in the size range of 100-1000 μ can be produced in the near future.

The shattering of liquid drops is considered to be an important phenomenon in spray detonations. For this reason an experimental shock tube setup for the study of this phenomenon under conditions expected in detonations is designed and described. These conditions are in the Reynolds and Weber number ranges beyond those attained in the past for similar studies.

LIST OF FIGURES

LIST OF FIGURES (cont)

LIST OF TABLES

NOMENCLATURE

a	Speed of sound
C	Coefficient of contraction
C_D	Drag coefficient
c_p	Specific heat at constant pressure
D	Drop diameter
d_j	Jet diameter
d_s	Diameter of source
e_ℓ	Internal energy of liquid
f	Frequency
f_c, f_1	Focal lengths
g	Acceleration due to gravity
h	Enthalpy
I	Object size
I_0, I_1	Modified Bessel functions of first kind and zeroth or first order
ΔI	Increment in object size
L	Tube length
M	Mach number
M	Magnification
m	Molecular weight
N	Number density
n	Fuel-oxidizer mole ratio for stoichiometric mixture
p	Pressure
Δp	Pressure drop

NOMENCLATURE (cont)

Q	Volumetric rate per unit area
Q	Heat release plus internal energy of drops
$\overline{Q}$	Heat release due to chemical reaction and phase change
q	Amplification parameter
R_0	Universal gas constant
Re	Reynolds number = $\rho VD/\mu$
r	Radius
Δr	Change in jet radius
Δs	Depth of focus
T	Temperature
u	Velocity
$\overline{u}$	Average velocity
V	Velocity
We	Weber number = $\rho V^2 D/\sigma$
z	Jet axis
α	Total mass per unit mass of the gaseous component of a two phase mixture
γ	Ratio of specific heats
λ	Wavelength
μ	Viscosity
ρ	Density
ρ_ℓ'	Density of liquid based on unit volume of mixture
σ	Surface tension
ϕ	Equivalence ratio

Subscripts

1, 2	Condition ahead and behind wave
4	Driver condition
D	Diaphragm section
g	Gas, or all-gaseous case
j	Jet
ℓ	Liquid
s	Shock
t	Tube

I. INTRODUCTION

In recent years, large liquid propellant rocket motors have been beset with the serious problem of combustion instability. These instabilities have been experienced in all of the three possible modes; the radial, longitudinal, and the tangential. The latter mode is usually the most serious (sometimes catastrophic) of the three with chamber pressure excursions of many hundreds of pounds per square inch being experienced. Considerably smaller pressure fluctuations than this are sufficient to cause mission failure in some cases. The understanding of the combustion instability problem is far from complete; the complexity of the problem precluding an all inclusive theoretical approach. In fact, even resort to a testing program guided by the appropriate similarity (scaling) parameters has not been too fruitful because of the large number of these parameters and the consequent inability to test the influence of one parameter at a time. Accordingly, it has been necessary to conduct exhaustive experimental programs on relatively large, and sometimes full, scale motors. In addition there have been studies on small scale motors wherein isolated aspects of the overall problem have been emphasized. The difficulty here is, of course, in scaling up the results to the large motors. Isolated aspects of the problem have also been treated analytically.

For the most part, the combustion instability problem has been treated as an acoustic problem. In recent years more attention has been given to the possibility of non-linear phenomena, i. e., shock waves coupled to the combustion process. The question then arises as to whether detonation or "detonation-like" waves play a role in

rocket motor combustion instability. This is a difficult question to resolve on the basis of motor tests because of the complicated fluid dynamic processes in the motor and the severe instrumentation problems. However, some recent experimental results on a relatively large (18 in. I. D.) liquid motor are significant. Utilizing a number of high frequency response pressure transducers located in the wall at varying axial positions, Rupe et al.[1] have determined that a strong, steep wave is rotating around the motor at a very stable constant velocity. The pressure ratio across the wave tends to increase near the injector plate and to decrease in the direction of the nozzles. Their conclusion is that this must be a detonation or detonation-like wave.

The motivation for the work reported here centers around the question as to whether detonation plays a role in rocket motor combustion instability or not. Towards this end we have embarked on a study of heterogeneous (two-phase) detonation. The progress in the first year is reported herein.

The problem of heterogeneous detonation has received relatively little attention to date. Williams[2, 3], in an analytical treatment of the problem, concluded that two phase detonations would be impossible because of the extended reaction zone arising from the leisurely droplet evaporation processes. However, he tempered his conclusions with two observations; first, that drops below about 10 microns would produce essentially a gas phase detonation, and second, that drop shattering might circumvent the slow evaporation processes and thus support detonation. Webber[4] and Cramer[5] conducted some preliminary experiments by using a combustion driven shock tube to

pass a shock wave through a diethylcyclohexane (DECH) spray in an oxygen atmosphere. These experiments resulted in a steep fronted high velocity wave which Cramer termed "detonation-like."

The above studies still leave many unanswered questions regarding the possibility of detonation in two phase systems and a systematic theoretical-experimental program is in order. Ideally one would like to:

a) generate a spatially homogeneous mixture of a gaseous oxidizer (or fuel) and uniform size liquid fuel (or oxidizer) drops,

b) pass a shock wave of known and controllable strength into this mixture, ensuring that the test time between the shock and gaseous interface is adequate for the purpose at hand,

c) measure and photograph the results with suitable time resolved instrumentation,

d) conduct a theoretical analysis of the model, and

e) combine the theoretical and experimental treatment to arrive at conclusions concerning the onset and propagation of heterogeneous detonation if at all possible.

Unfortunately such an idealized approach cannot be immediately adopted largely because of the inability to generate a monodisperse system of liquid drops. Accordingly the approach that has been adopted is to proceed along three parallel paths. One phase has been to use a refined version of Cramer's technique to study the passage of shocks over a DECH spray in gaseous oxygen. A theoretical treatment proceeds simultaneously with this. A second phase has been devoted to an attempt to generate a homogeneous monodisperse drop field. The

third effort is concerned with the shattering of liquid drops in high velocity streams. These phases are discussed individually in the ensuing sections. A section devoted to future plans is also included.

II. TWO PHASE DETONATION

1. Theoretical Aspects

To assess some features of the propagation of detonation waves through a heterogeneous medium wherein the fuel or oxidizer exists in the form of liquid droplets, it is appropriate to rederive the jump relations for the spray detonation which were first obtained by Williams[2] using an idealized model of the actual relevent processes. The objective here is to include molecular and ratio of specific heat effects and to obtain typical numbers for our experiments. As in Williams' work the results will be derived in forms useful for obtaining comparisons between spray and all-gaseous detonations.

The basic assumptions employed in deriving the hydrodynamic jump relations for an idealized spray detonation wave are as follows.

(1) The spray is dilute: the volume occupied by the liquid droplets is very much less than the volume of the surrounding gas. (For the DECH-O_2 system investigated experimentally under this study the volume ratio is of order 10^{-3}.)

(2) The mass of the droplets is initially uniformly distributed in space, and the droplets travel with the same velocity as that of the gas.

(3) At the end of the combustion zone the liquid droplets are completely disintegrated to produce a uniform mixture of burned gases.

(4) The Chapman-Jouguet condition is satisfied: the velocity of the products of combustion is sonic relative to the moving detonation wave.

(5) All the gases present are thermally and calorically perfect.

The conservation equations across a discontinuity for a spray can readily be written if the parameter

$$\alpha = 1 + \rho_\ell'/\rho_1$$

is introduced. This parameter is the sum of the mass of the liquid and the gas per unit mass of the gaseous component. (In Williams' notation $\alpha = 1/(1 - z_0)$ where z_0 is the mass fraction of the liquid component.)

Conservation of mass:

$$\rho_2 V_2 = \alpha \rho_1 V_1 \tag{1}$$

Conservation of momentum:

$$p_2 + \rho_2 V_2^2 = p_1 + \alpha \rho_1 V_1^2 \tag{2}$$

Conservation of energy:

$$\alpha \left(h_2 + \frac{1}{2} V_2^2 \right) = h_1 + \frac{\alpha}{2} V_1^2 + (\alpha - 1)\, e_\ell \tag{3}$$

These equations together with the Chapman-Jouguet condition:

$$V_2 = a_2 \tag{4}$$

and the ideal gas relationships:

$$\left.\begin{aligned} h_1 = c_{p1} T_1 \quad , \quad h_2 = c_{p2} T_2 - \overline{Q} \\ p = \rho R_0 T/m \quad , \quad a^2 = \gamma p/\rho \\ c_p = \gamma R_0/(\gamma - 1)m \end{aligned}\right\} \tag{5}$$

can be used to derive the jump conditions. $\overline{Q}$ is the heat released per unit mass of mixture due to chemical reaction and change of phase in the heterogeneous detonation process.

The energy equation can be simplified by defining:

$$Q = \overline{Q} + (\alpha - 1)\, e_\ell/\alpha \tag{6}$$

to obtain:

$$c_{p2}\, T_2 + \frac{1}{2} V_2^{\,2} = \frac{1}{\alpha} c_{p1}\, T_1 + \frac{1}{2} V_1^{\,2} + Q \tag{3a}$$

To carry out the solution of these equations in a convenient manner, we introduce the Mach number $M = V/a$. Then, from Eq. (1), (2), (3a) and (4) and (5) we have:

$$\alpha M_1^{\,2} = \frac{\gamma_2^{\,2} - 1}{\gamma_1 - 1}\left(1 + \frac{\alpha Q}{c_{p1}\, T_1}\right) - \frac{\gamma_2^{\,2}}{\gamma_1} + \sqrt{\left[\frac{\gamma_2^{\,2} - 1}{\gamma_1 - 1}\left(1 + \frac{\alpha Q}{c_{p1}\, T_1}\right) - \frac{\gamma_2^{\,2}}{\gamma_1}\right]^2 - \frac{\gamma_2^{\,2}}{\gamma_1^{\,2}}} \tag{7}$$

$$p_2/p_1 = (1 + \alpha\gamma_1 M_1^{\,2})/(1 + \gamma_2) \tag{8}$$

$$\rho_2/\rho_1 = \alpha^2 \gamma_1 (1 + \gamma_2)\, M_1^{\,2}/\gamma_2 (1 + \alpha\gamma_1 M_1^{\,2}) \tag{9}$$

$$T_2/T_1 = \gamma_2 m_2 (1 + \alpha\gamma_1 M_1^{\,2})^2 /\gamma_1 m_1 (1 + \gamma_2)^2\, \alpha^2 M_1^{\,2} \tag{10}$$

These equations for spray detonations are similar to those for the all-gaseous detonation relations which can readily be written by setting $\alpha = 1$.

To obtain simple relationships between the jump relations in the two cases we use the following approximations:

(1) The heat released per unit mass due to chemical reaction is much greater than the initial static enthalpy of the gases:

$$\frac{Q}{c_{p1} T_1} \gg 1 \quad , \quad \frac{Q_g}{c_{p1g} T_{1g}} \gg 1$$

(Subscript g is used for the all-gaseous case.) From equation (7) it can be seen that this condition is equivalent to the requirements

$$M_1^2 \gg 1 \quad , \quad M_{1g}^2 \gg 1$$

The error introduced by this approximation amounts, for all-gaseous detonation waves, to about 3 to 6%.

(2) The specific heat ratios and molecular weights for the final state of the gases are approximately equal in the two cases:

$$\gamma_{2g} \approx \gamma_2 \quad , \quad m_{2g} \approx m_2$$

This assumption would seem to be reasonable if the initial constituents and the fuel-oxidizer ratio are comparable for the spray and the all-gaseous detonation waves.

Application of these approximations to Eq. (7-10) and their counterparts for the all-gaseous case, yields:

$$M_1/M_{1g} \simeq (\gamma_{1g} m_1 Q T_{1g} / \gamma_1 m_{1g} Q_g T_1)^{1/2} \tag{11}$$

$$V_1/V_{1g} \simeq (Q/Q_g)^{1/2} \tag{12}$$

$$\frac{p_2/p_1}{(p_2/p_1)_g} \simeq \frac{\alpha m_1 Q T_{1g}}{m_{1g} Q_g T_1} \tag{13}$$

$$\frac{\rho_2/\rho_1}{(\rho_2/\rho_1)_g} \simeq \alpha \tag{14}$$

$$\frac{T_2/T_1}{(T_2/T_1)_g} \simeq \frac{Q T_{1g}}{Q_g T_1} \tag{15}$$

Williams[2], who makes a similar analysis, except with constant specific heat ratio and molecular weight across the detonation wave, concludes that for a given value of $\overline{Q}/c_{p1}T_1$ a Chapman-Jouguet detonation in a spray propagates at a slightly higher Mach number (M_1) and has a higher pressure and temperature downstream than does a gaseous detonation with the same heat release and the same initial pressure, temperature, and gas density. However, aside from the effect of the Q/Q_g ratio, the present study indicates a significant effect due to initial molecular weight and specific heat ratio changes. For example, consider the predictions for the following two systems where $Q/Q_g \equiv 1$ is used, and where the initial temperatures of the spray and the all-gaseous cases are assumed identical. The assumption that $Q = Q_g$ is reasonable since they effectively differ by the latent heat of vaporization of the liquid which is usually less than 1% of Q.

Mixture	$C_{10}H_{20} + 15\ O_2$	$2H_2 + O_2$
spray	liquid $C_{10}H_{20}$, gaseous O_2	liquid O_2 gaseous H_2
γ_1	1.4	1.4
γ_{1g}	1.28*	1.4
m_1	32	2.0
m_{1g}	38.75	12
α	1.292	9
M_1/M_{1g}	.861	.408
V_1/V_{1g}	1.0	1.0
$(p_2/p_1)/(p_2/p_1)_g$	1.069	1.5
$(\rho_2/\rho_1)/(\rho_2/\rho_1)_g$	1.292	9.0

These examples show that the molecular weight effect can be significant.

2. Experimental Studies

Heterogeneous detonation experiments were conducted using gaseous oxygen and liquid fuel which was in the form of droplets produced from spray nozzles. In order to generate the shock wave a combustion driven shock tube shown pictorially in Fig. 1 was used. Diethylcyclohexane (DECH) was chosen as the fuel because of its low vapor pressure and because it is a pure compound with properties very similar to RP-1. The physical properties of DECH are shown in Tables 1 and 2. In the experiments conducted the velocity and pressure of the wave processes within the combustion tube were measured as a function of time and position. Also self-luminous as well as spark schlieren photographs were taken. This work, therefore, continues the experiments

*Obtained by assuming $\gamma = 1.1$ for gaseous DECH.

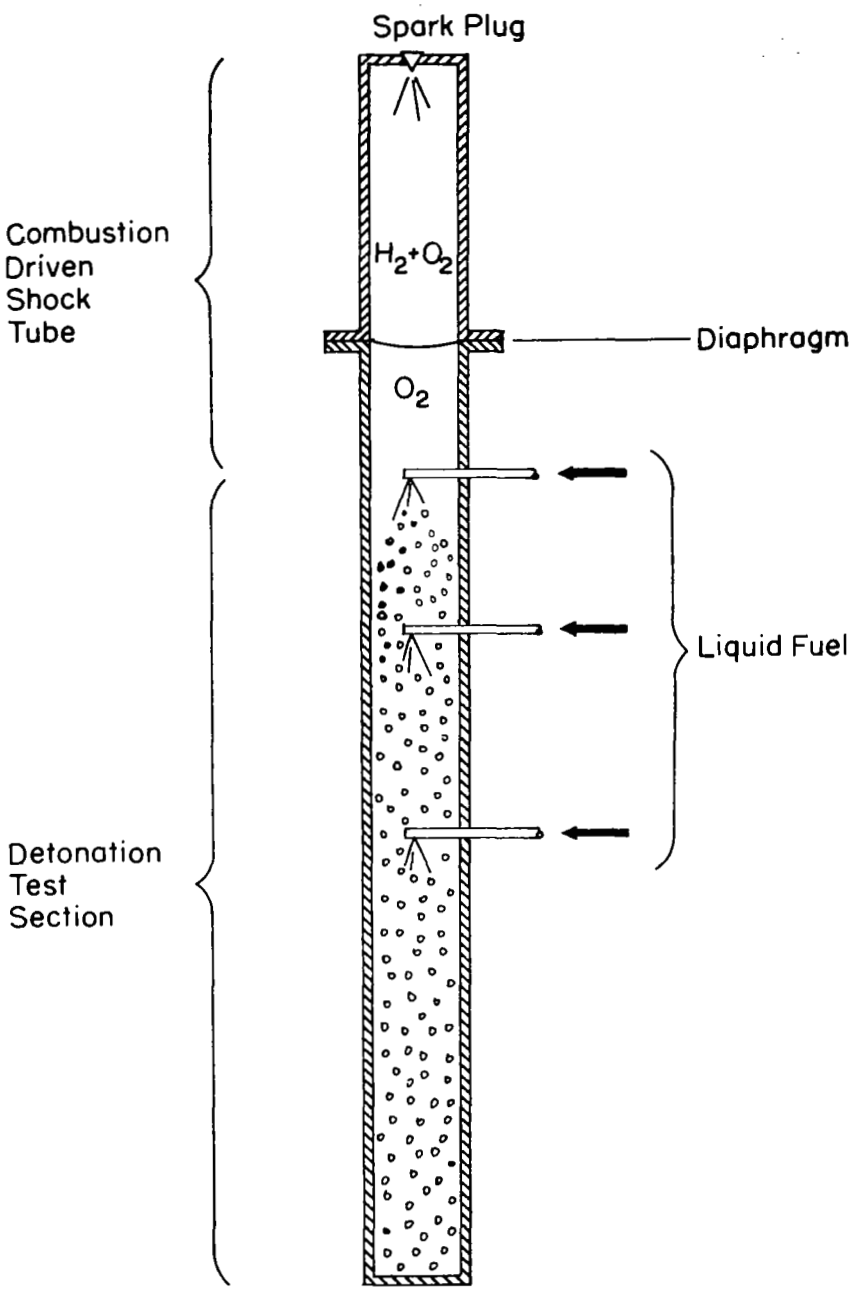

Figure 1. Schematic Diagram of the Combustion Tube.

Table 1. Physical Properties of Diethylcyclohexane[6, 7]
(Mixed Isomers)

Formula: $C_{10}H_{20}$

Structure:

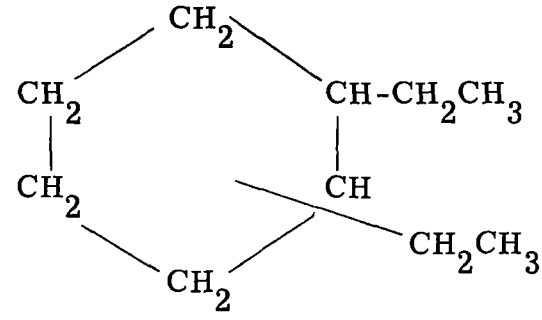

Molecular weight: 140.3

Approximate Assay:

Diethylcyclohexane (mixed isomers)	98.0% (wt)
Other C_{10} cyclic hydrocarbons	1.4
C_9 cyclic hydrocarbons plus paraffins	0.6
Aromatics (by ultraviolet):	0.12%

Freezing point: $-75^{\circ}F$

Boiling point: $346^{\circ}F$

Decomposition temp.: $744^{\circ}F$

Heat of vaporization*: 139 Btu/lb

Heat of combustion: 18,650 Btu/lb

Heat capacity: 0.443 Btu/lb $^{\circ}F$ at $100^{\circ}F$

Thermal conductivity: 0.0588 Btu/hr ft^2 $^{\circ}F/ft$ at $219^{\circ}F$

Kinematic viscosity: 4.41 cs at $-30^{\circ}F$
1.07 cs at $100^{\circ}F$
0.57 cs at $210^{\circ}F$

*Indicates properties are for 1, 1-diethylcyclohexane.

Table 1 (cont)

Critical temperature: 1153°F

Critical pressure: 25.0 atm

Vapor pressure: 1.45 mm Hg at 70°F (estimated, see Table 2)

Surface tension[8]: 27.0 dynes/cm

Vapor phase properties:

Heat capacity	0.637 Btu/lb °F at 600°F
	0.681 Btu/lb °F at 700°F
	0.720 Btu/lb °F at 800°F
Thermal conductivity	0.0233 Btu/hr ft^2 °F/ft at 600°F
	0.0272 Btu/hr ft^2 °F/ft at 700°F
Viscosity	118 μp at 600°F
	128 μp at 700°F
	138 μp at 800°F

Table 2. Vapor Pressure of Diethylcyclohexane

Temperature °F	Vapor Pressure - mm Hg		
	Cox Chart for C_{10} Compounds (Ref. 9)	1, 1-diethyl-cyclohexane (Ref. 7)	Mixed Isomers diethylcyclohexane (Ref. 7)
70	1.45		
200	62.0	46	
250	155	130	
300	413	370	
346			760
350	826	760	

conducted by Webber[4] and Cramer[5], and their geometry was followed closely with the important difference that the combustion process was initiated by a plane normal shock which was well separated from the driver gases. In carrying out the work a rather new and unexpected phenomenon was uncovered. Namely, in the absence of spray but with the walls of the combustion tube wetted with a thin layer of DECH, a combustion-shock interaction was observed. The equipment and instrumentation used in the spray and wet-wall tests will now be described and then the test results presented and discussed.

The test equipment for the heterogeneous detonation experiments consisted of two different combustion tubes (one of circular cross-section for spray detonation studies and one of square cross-section for optical combustion studies), spray injectors, a gas flow control system, and an electrical sequence control setup.

The combustion tube with circular cross-section has an inside diameter of 2.0 in., the driver section is 48 in. long and the test section 96 in. long. In the tests to date the plane shock was generated by using a detonation wave in the driver. Low pressure stoichiometric hydrogen-oxygen (1/2 to 1 atm) was detonated; the detonation wave impacts on the diaphragm and a normal shock is transmitted into the test section followed at a later time by the hot gases from the driver. Details of the flow pattern are given later. The combustion tube is mounted vertically with the driver above the test section. A photograph of the circular combustion tube is shown in Fig. 2. It is made of 2 in. I. D. seamless 304 stainless steel with 1/4 in. walls. The second combustion tube which was used for the optical studies, utilized the same 2 in. I. D. driver section; the test section had an inside cross-section of 1.64 by 1.64 in. with 1/4 in. walls and was made of welded

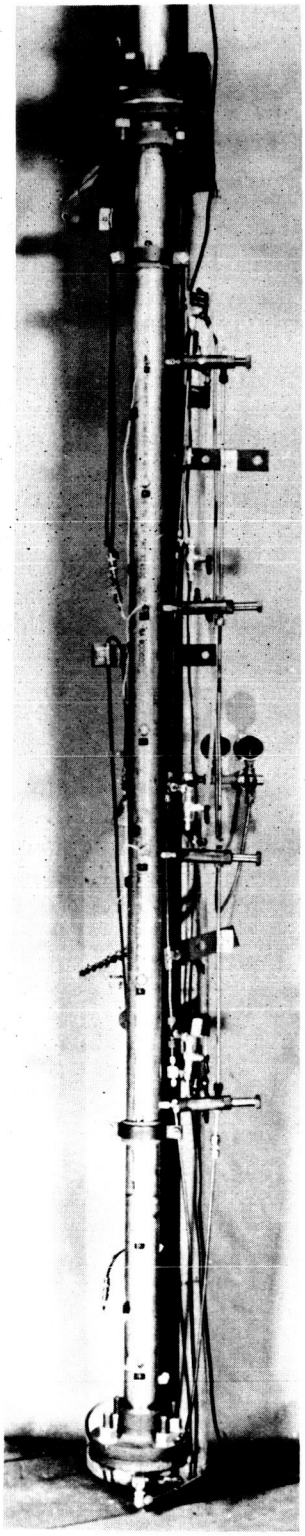

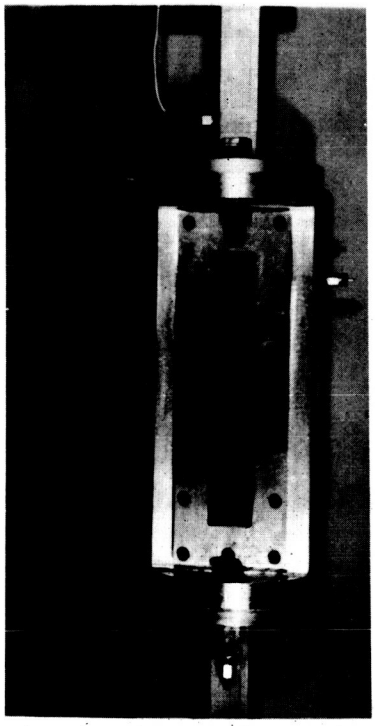

Figure 2. Photographs of the 2.0 Inch Diameter Combustion Tube and the 1.64 by 1.64 Inch Optical Test Section.

1020 steel and was hard chrome plated. The optical section, which is shown in Fig. 2, was made from a 2024-T4 aluminum billet. The diaphragm material used throughout the tests was 0.001 in. Mylar.

The injector design, which is shown in Fig. 3, follows very closely that used by Cramer[5]. The liquid fuel was forced downward through a 0.022 diameter hole by a piston which was actuated by nitrogen gas at 150 psi. Each of the four injectors was loaded without removal from the test section by a gravity feed with the piston fully retracted. After a test run the piston was returned to the initial position by applying nitrogen pressure as shown in Fig. 3. To obtain an idea of the extent of the spray, the unconfined spray was photographed with a General Electric electronic flash of 1 microsecond duration, front lighted, with 3000 ASA Polaroid film. Nitrogen pressure was applied rapidly by means of a solenoid valve and at a measured time delay later the flash was actuated. Two such photographs obtained in this manner are shown in Fig. 4. On the basis of these tests it was concluded that 150 psig nitrogen pressure and a 275 millisecond delay after opening of the solenoid valve would be reasonable for use in the combustion tube. Under these conditions the spray extends at least three feet with the larger drops predominately in the last foot. While a large portion of the spray is contained within a 2 in. diameter, the pictures indicate that the walls of the combustion tube would also be heavily wetted. No attempt was made to measure the size distribution of the droplets in the spray. Cramer[5] using a similar injector reports a near normal distribution with a mean diameter of 200 microns for his spray.

The injectors that were used were located 18 in. apart along the driven section as indicated in Fig. 5 and each sprayed downward. Thus no fuel was present in the first 18 in. of the test section.

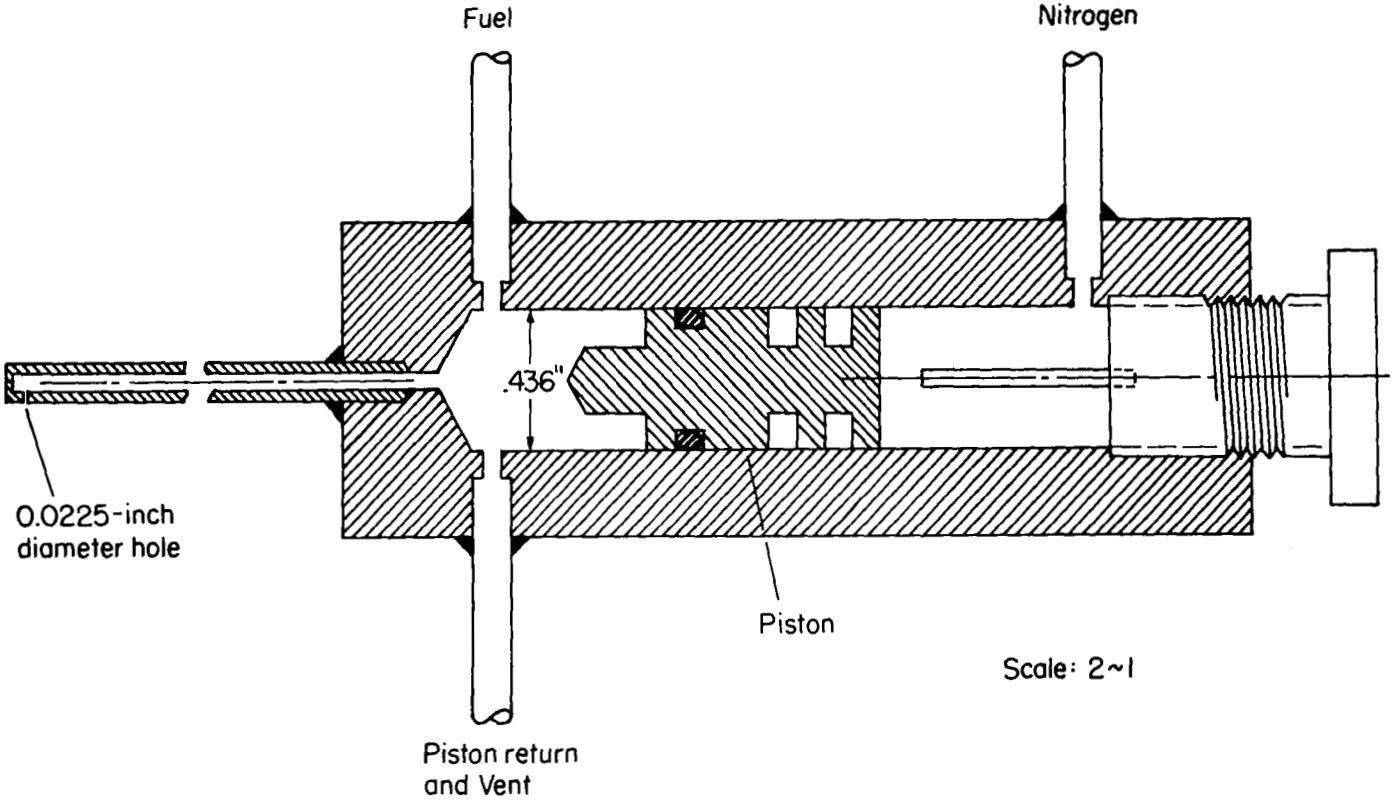

Figure 3. Fuel Injector.

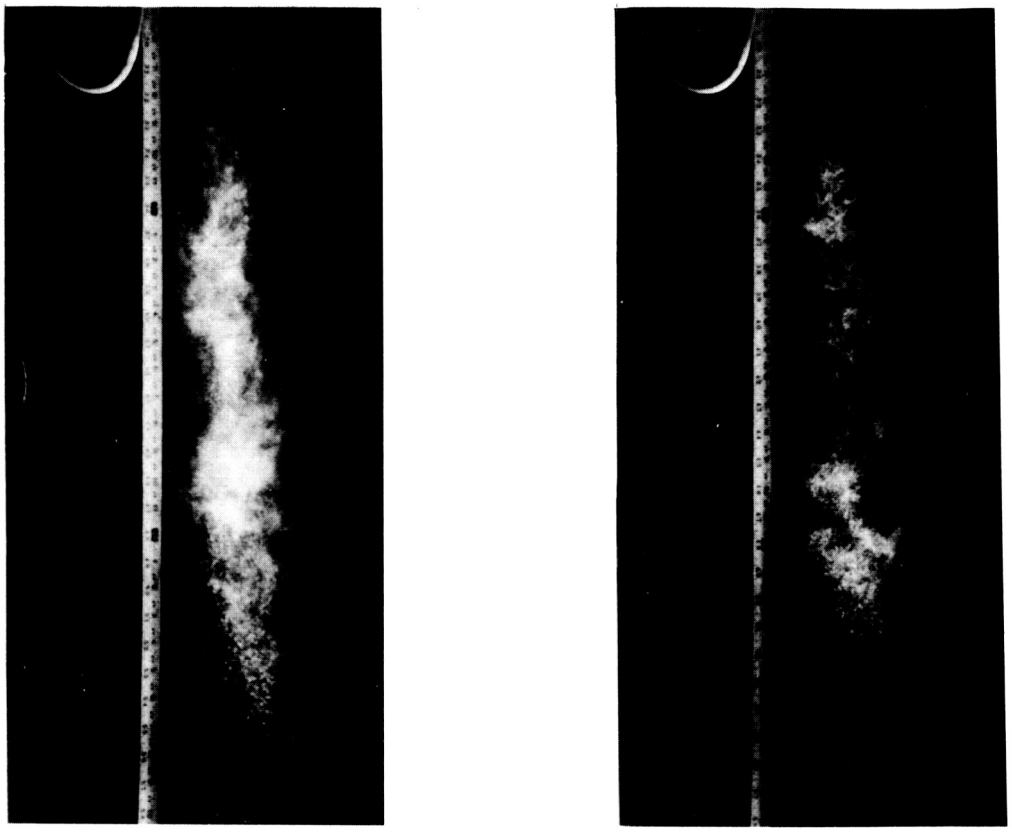

(a) 200 psig
190 millisec delay

(b) 150 psig
275 millisec delay

Note: the orifice is located at the 2 foot mark

Figure 4. 1 Milliliter DECH Spray (0.0225 inch diameter orifice)

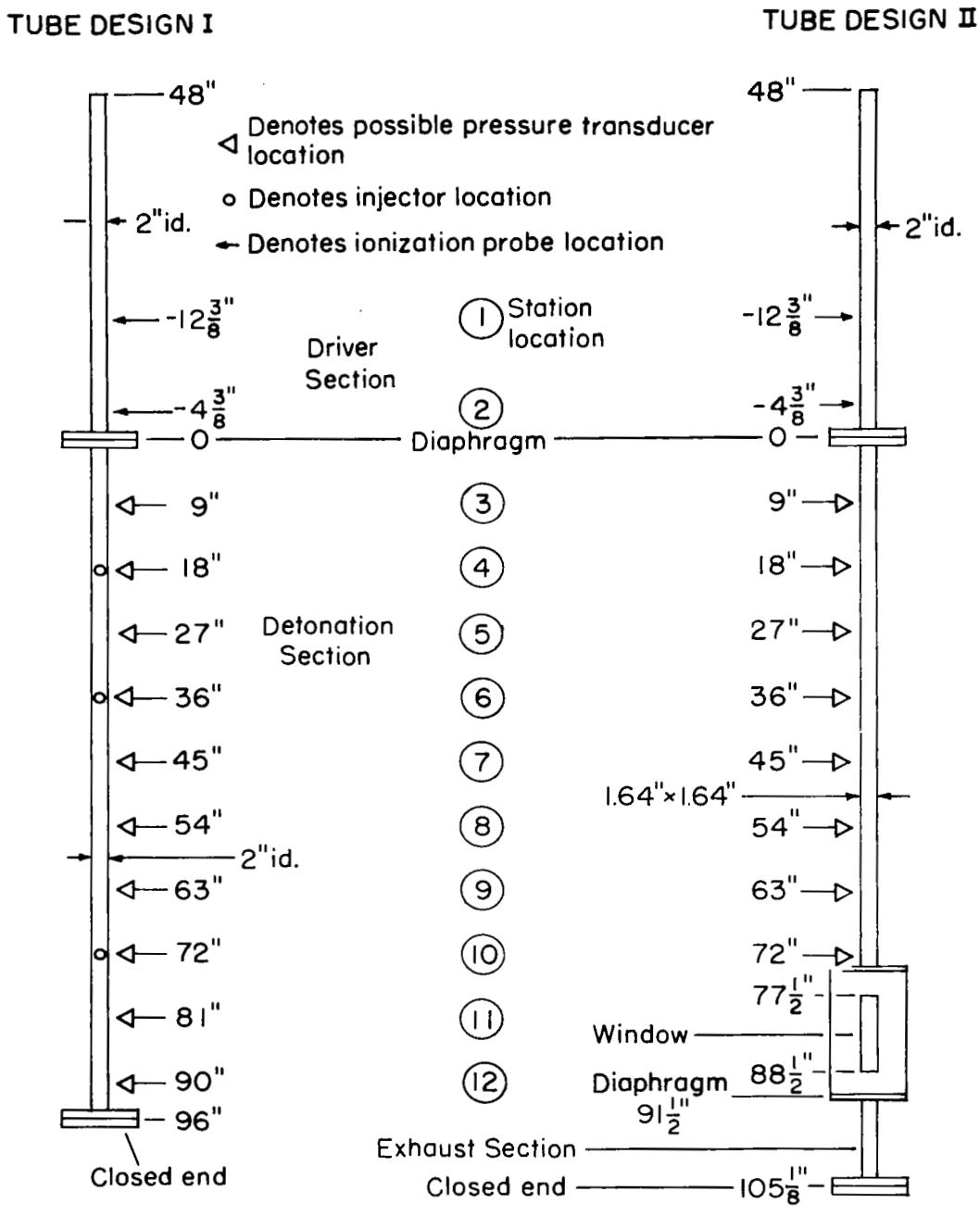

Figure 5. Location of Probes and Injectors in the Detonation Tubes.

The sequence of events in making a test run in the combustion tube was as follows:

1. Blow back the injector pistons.
2. Replace the diaphragm and evacuate the driver and the test section.
3. Fill the test section with oxygen.
4. Load the injectors.
5. Fill the driver with premixed hydrogen-oxygen.
6. Fire the injector solenoid valves.
7. 275 msec later the spark plug fires in the driver section.
8. Instrumentation is triggered by ionization probe in the driver section.

The system used to meter the gas flow to the combustion tube is shown in Fig. 6 and the electrical sequence control unit is shown in Fig. 7.

The instrumentation consisted of pressure transducers to measure the velocity and pressure of the waves in the combustion tube, ionization probes to sense the detonation wave in the driver, and a high speed framing camera and a spark schlieren setup. Two Kistler 603 and two Kistler 601A pressure transducers were flush-mounted in the combustion tube. The output from the transducers was amplified by Kistler 566 electrostatic charge amplifiers and then displayed on a Tektronix 555 dual beam oscilloscope. Before using the pressure transducers their response to a hydrogen-oxygen detonation wave in a 1/2 x 3/8 tube was checked. The theoretical peak pressure agreed very well with the manufacturer's static calibration, and the rise time was 1-3 microseconds. The pressure signal from the transducers oscillates

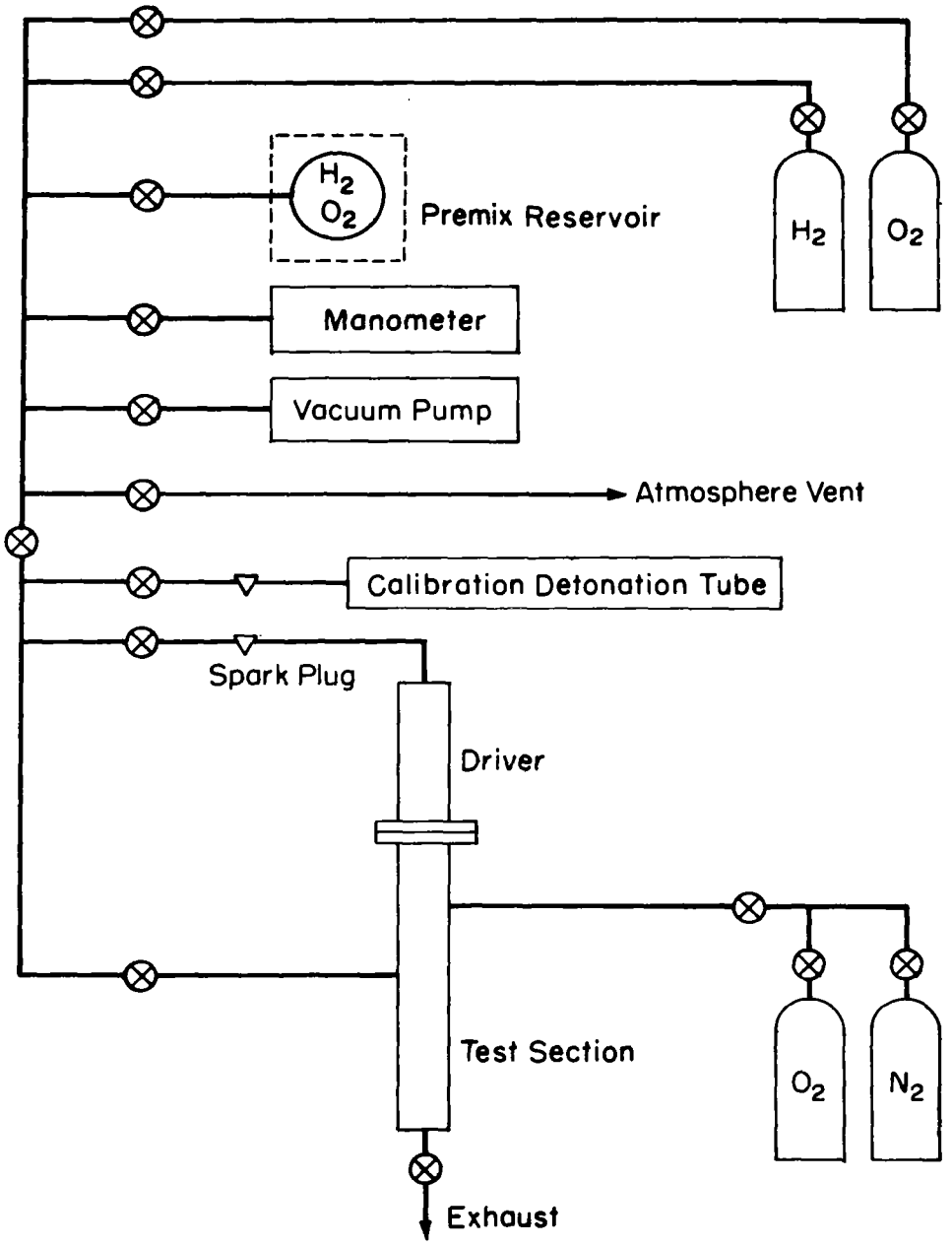

Figure 6(a). Gas Flow Control System.

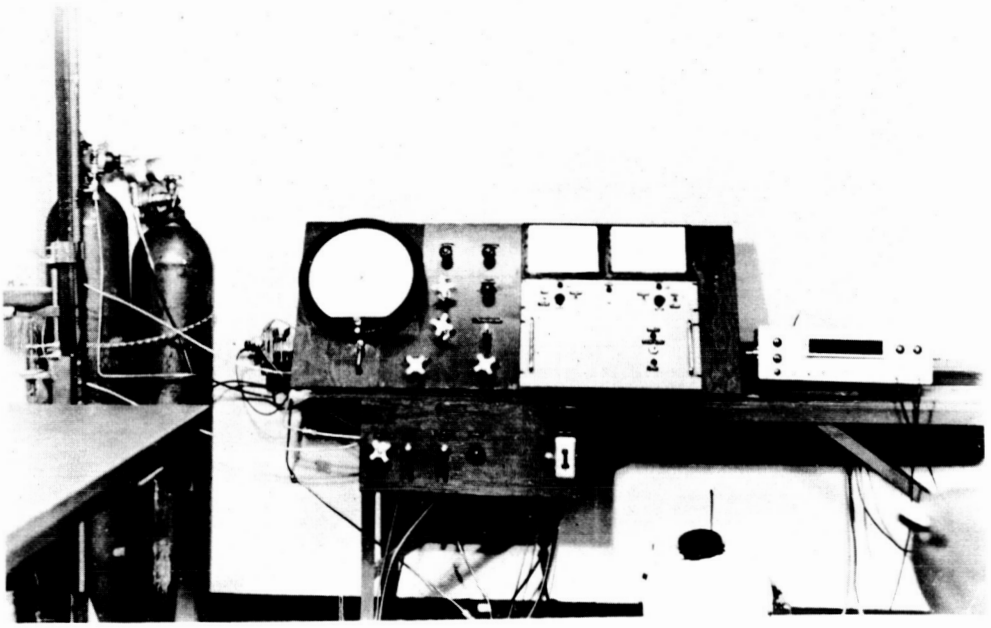

Figure 6(b). Gas Flow Control System

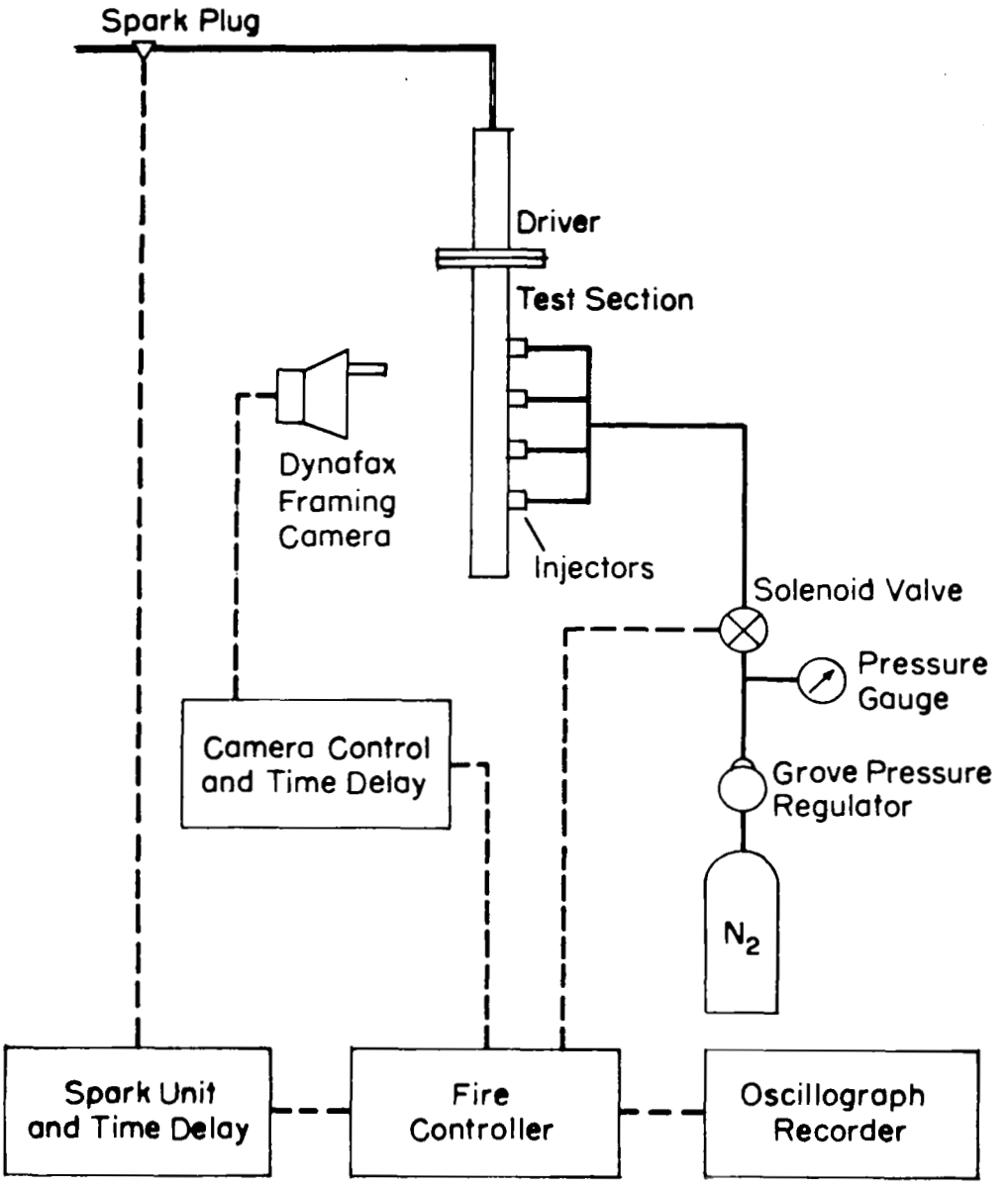

Figure 7(a). Electrical Sequence Control System.

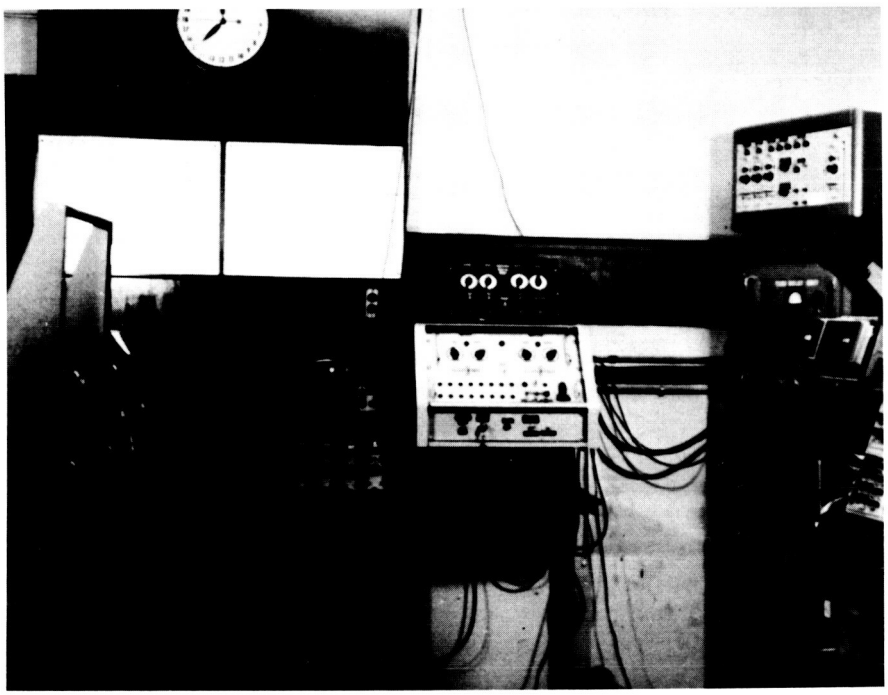

Figure 7(b). Electrical Sequence Control System

ratherly badly due to external vibration and ringing within the crystal itself. Pressure waves transmitted in the walls of the combustion tube which arrive ahead of the flow inside the tube are also superimposed on the gasdynamic pressure as can be observed for example in Fig. 9. It was decided, however, not to damp the transducer signal electronically or mechanically in order to preserve the short rise time of the pickups. Ionization probes in the driver were used to check the performance of the driver and to trigger the sweep on the oscilloscope for the pressure recordings. The station location of the pressure transducers and ionization probes is shown in Fig. 5. Photographs were taken through the optical test section with the Beckman and Whitley Framing Camera Model 326 which was operated at its maximum speed of 26,000 frames per second and at the minimum exposure time of 1 microsecond per frame. Kodak Tri-X film developed in Baumann Diafine was used. Spark schlieren photographs were also taken using an end-fire spark gap utilizing ten 500 $\mu\mu$f capacitors which were charged to 28 kilovolts. The estimated duration of light is 0.2 microseconds. The optical setup consisted of a condensing lens for the light source, an 8 in. diameter f 5.3 collimating mirror, a 6 in. diameter f 8.7 focusing mirror, a circular hole of 0.052 diameter as a knife edge, a Kodak blue filter (No. 47B), and finally 3000 ASA Polaroid film. The circular hole cut-off and the filter were used in order to minimize the exposure from the direct-luminosity of combustion.

3. Test Results and Discussion

The performance of the driver, which provides the initial conditions for the test section, is now presented. A shock wave is transmitted into the test section when the hydrogen-oxygen detonation in

the driver strikes the diaphragm. At the same time a shock is reflected backwards off the diaphragm, strikes the end of the driver and then propagates down the tube behind the initial shock. In addition the interface separating the shocked oxygen and the hot hydrogen-oxygen driver gases follows the initial shock at a somewhat lower velocity. For a one atmosphere $2H_2 + O_2$ detonation into one atmosphere O_2 theory predicts (Ref. 10) a transmitted shock Mach number of 4.5. Measurements such as from Fig. 8 and Table 3 indicate that the shock Mach number at 1.5 ft from the diaphragm is about 4.1. The theoretical velocity of the interface between driver and test section gases is 3400 ft/sec, so that a uniform flow behind the shock exists for 120 microseconds theoretically at a distance of 1.5 ft where the fuel is first available. The reflected shock off the end of the driver does not arrive at the 1.5 ft station until 1000 microseconds after the initial shock and thus need not be considered further. (The second reflected shock shown in Fig. 8, which arrives about 500 μsec after the first reflected shock, may be due to the non-uniformity of the driver gases but again is not important for the experiments.) The incident normal shock at the 1.5 ft section thus determines the initial conditions for the experiments.

Since the pressure behind the detonation wave in the driver decays the pressure of the transmitted shock is not a step function but rather a decaying one. The one-dimensional shock relations give the peak conditions which, for a Mach 4.1 shock, are as follows:

Peak Temperature	$2180^{\circ}R$
Convective Velocity	3340 ft/sec
Peak Pressure	293 psia

When nitrogen is used in the test section the initial shock Mach number is reduced rather rapidly as it progresses down the test section due to

Transmitted Shock in 1 Atm N_2

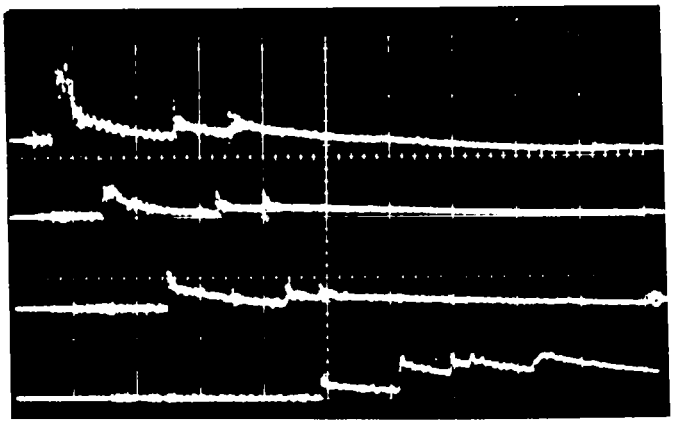

Transmitted Shock in 1 Atm N_2 plus
2 ml DECH Spray

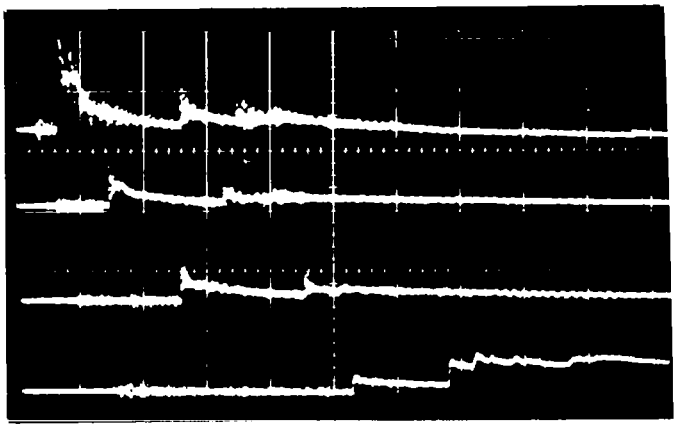

Figure 8. Pressure Traces of Transmitted Shock in Nitrogen and Nitrogen Plus DECH Spray (1 Atm $2H_2 + O_2$ in Driver)

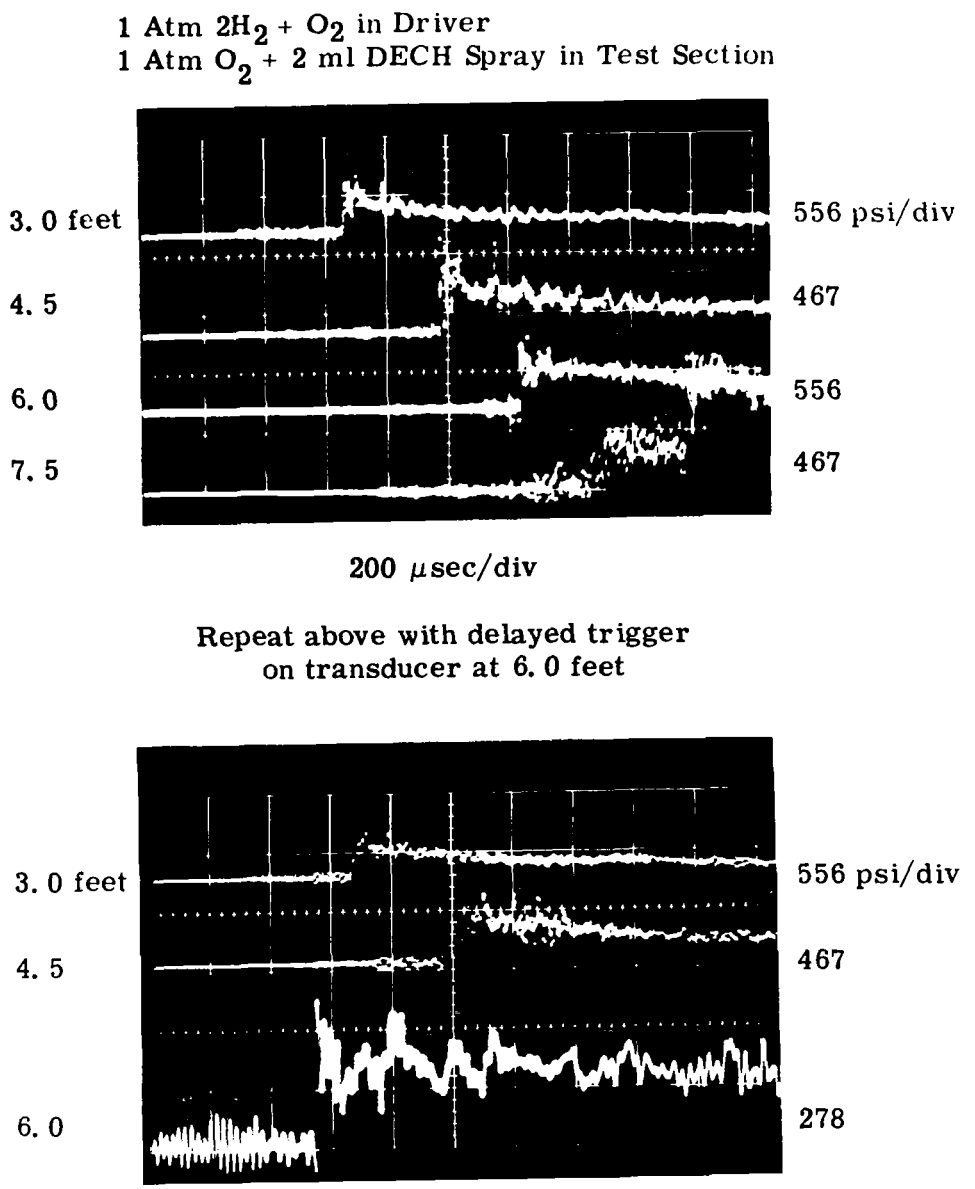

Figure 9. Pressure Traces of Detonation in Oxygen—DECH Spray (1 Atm $2H_2 + O_2$ in Driver, 1 Atm O_2 + 2 ml DECH in Test Section)

Table 3. Summary of Test Runs Data

(1) Type of Run	(2) Run No.	(3) Transducer Station	(4) P_2 (Transducer Pressure, psia)	(5) P_2/P_1 (Across Wave)	(6) Time (μsec)	(7) Velocity (ft/sec)
1 atm $2H_2 + O_2$	A	2			0	
1 atm N_2	(Typical)	4	293	19.3	320	4000
		6	154	10.1	700	3160
		8	127	8.3	1175	2500
		12	71	4.7	2375	
1 atm $2H_2 + O_2$	B	2			0	
1 atm N_2 +	(Typical)	4	293	19.3	320	3750
2 mℓ DECH spray		6	130	8.5	720	2860
		8	99	6.5	1245	2260
		12	62	4.1	2565	
1 atm $2H_2 + O_2$	1	2			0	
1 atm O_2 +		3			150	4690
2 mℓ DECH spray		4	237	16.1	310	4690
		5	295	20.0	470	4280
		6	340	23.1	645	
	2	2			0	
		3			145	4690
		4			305	4690
		5			465	4280
		6			640	
	3	2			0	
		6	405	27.6	680	4690
		8	482	32.8	1000	5750
		10			1260	5750
		12			1520	

Table 3 (cont)

(1)	(2)	(3)	(4)	(5)	(6)	(7)
	4	2			0	
		6	459	26.5	610	5170
		8	482	32.8	900	5750
		10	459	31.2	1160	5360
		12	482	32.8	1440	
	5	2			0	
		6	405	26.7	650	5000
		8	459	30.1	950	5350
		10	460	30.1	1230	5350
		12	435	28.6	1510	
	6	2			0	
		6	411	28.0	650	4840
		8	437	29.7	960	5460
		10	460	31.3	1235	
	7	2			0	
		6	348	23.7	650	5170
		8	388	26.4	940	5350
		10	359	24.4	1220	5760
		12			1480	
1 atm $2H_2 + O_2$ + 4 mℓ DECH spray	8	9			130	5770
		10				
	9	9			140	5350
		10				
	10	4			300	5000
		6				
	11	3			440	5100
		6				
	12	3			410	5400
		6				

Table 3 (cont)

(1)	(2)	(3)	(4)	(5)	(6)	(7)
1 atm $2H_2 + O_2$	13	2			0	
1 atm O_2 +		4	293	20.0	350	
12 mℓ DECH spray		6			650	5000
		8	340	23.2	925	5460
		12	389	26.5	1500	5220
1/2 atm $2H_2 + O_2$	14	2			0	
1 atm O_2 +		6	235	16.0	620	
2 mℓ DECH spray		8	435	29.6	920	5000
		10	468	31.8	1200	5350
		12			1480	5350
	15	2			0	
		4	235	16.0	900	
		6	293	19.9	1300	3750
		8	389	26.4	1675	4000
		12			2250	5220
1 atm $2H_2 + O_2$	16	2			0	
1 atm O_2 +		8	300	20.4	950	
12 mℓ DECH poured		10	364	24.8	1275	4620
on two walls	17	2			0	
		4			300	
		6	293	19.9	625	4620
		8	300	20.4	950	4620
		10	390	26.5	1275	4620
23 in. $2H_2 + O_2$	18	2			0	
1 atm O_2 +		4	182	12.4	250	
8 mℓ DECH poured		6			650	3750
on two walls		8	273	18.6	1000	4280
		12	335	22.8	1700	4280
26 in. $2H_2 + O_2$	19	2			0	
1 atm O_2 +		4	168	11.4	325	
4 mℓ DECH poured		6			725	3750
on two walls		8	202	13.7	1100	4000
		12	228	15.5	1900	3750

Table 3 (cont)

(1)	(2)	(3)	(4)	(5)	(6)	(7)
1 atm $2H_2 + O_2$	20	2			0	
1 atm O_2 +		4	290	19.7	325	3530
DECH swabbed		6	236	16.1	700	3750
on two walls		10	249	17.0	1500	
		Ten other runs very similar				
1 atm $2H_2 + O_2$	21	2			0	
1 atm O_2 +		4	290	19.7	325	3530
DECH swabbed		6	155	10.5	700	3160
on one wall		10	155	10.5	1650	
		Ten other runs very similar				

the expansion behind the shock front as shown in Fig. 8 and plotted in Fig. 10. When DECH spray (2 mℓ) is added to the test section the shock Mach number in N_2 is further reduced slightly as it progresses down the tube.

On the other hand when 2 mℓ of the fuel are sprayed into the test section containing O_2 the shock transmitted by the driver rapidly accelerates to a velocity of 5300 to 5700 ft/sec or a Mach No. of 5.0 to 5.2 based on the speed of sound of oxygen gas. The pressure jump across the wave was also increased to approximately 30 to 1. The results from various runs inferred from pressure traces represented by Fig. 9 are shown in Table 3, and plotted in Fig. 10. Two millileters of DECH represent a 1.2 stoichiometric mixture for the 2.0 in. diameter tube. While the gaseous DECH-oxygen Chapman-Jouguet detonation velocity is not accurately known, it is estimated to be approximately 8,000 ft/sec or Mach 7.2 for a stoichiometric mixture on the basis of Morrison's[10] experimental correlation for hydrocarbon fuels. Furthermore the measured pressure ratio of 30 to 1 is considerably higher than expected from one dimensional theory. For a plane heterogeneous Chapman-Jouguet detonation traveling at Mach 5.1 Eq. (8) predicts a pressure ratio of 21. Coincidentally the measured pressure ratio corresponds closely to a Mach 5 shock. One possible explanation is that the reaction zone may be of considerable extent so that heat release is not fast enough to lower the pressure.

Since the detonation velocity is considerably lower than the expected gaseous detonation velocity for a stoichiometric mixture it is possible that only a fraction of the fuel is entering into the initial reaction. Table 3 indicates that increasing the quantity of fuel sprayed into the

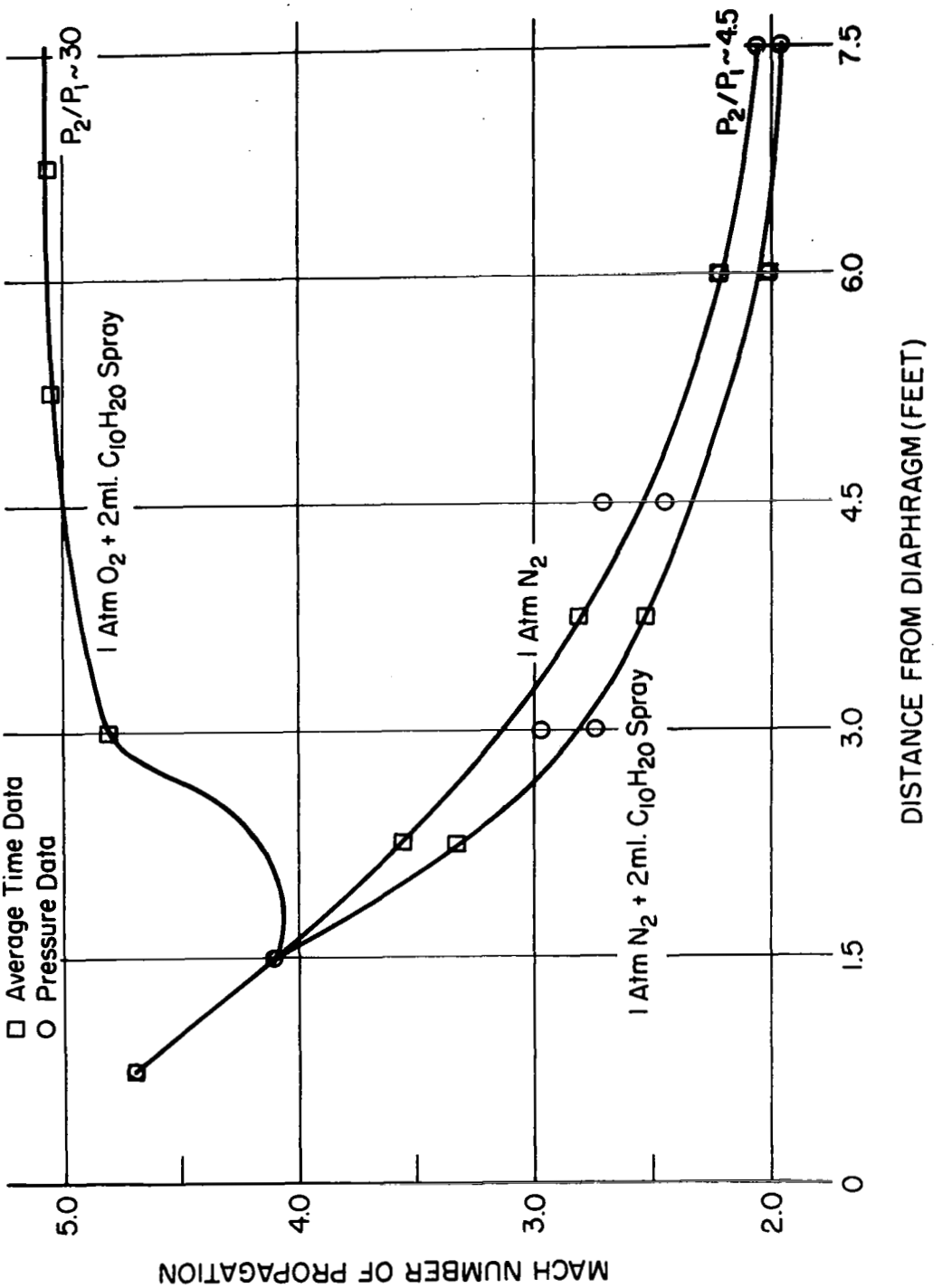

Figure 10. Plot of Mach Number vs. Distance from Figures 8 and 9.

test section did not significantly alter the results and that when the pressure in the driver was reduced to 1/2 atmosphere resulting in a Mach 3.7 shock at the 1.5 ft mark, the same qualitative results were observed.

At this point it should be mentioned that in the procedure of loading the injectors for a test run some fuel falls on the walls and wets the walls. It was felt initially that this procedure would be adequate inasmuch as the spray also wets the walls. Furthermore the fuel on the walls probably would not enter into the reaction soon enough anyway. However it was observed that when the injectors were loaded in the normal manner and a test run made in which the injectors were not fired, a combustion-shock interaction was still observed. Thus experiments were conducted in which the injectors were removed and a liquid layer of DECH was applied to the walls of the test section. The test section was then loaded with oxygen and results similar to the spray case were observed but with somewhat lower propagation velocities and pressure ratios.

In order to investigate this effect further an optical test section was built (see Fig. 2) and it was planned to take both self-luminous and schlieren photos of the spray and the wet-wall phenomena. To date pictures of the wet-wall reaction have been taken but pictures of the spray detonation have not yet been achieved due to the intense luminosity of the spray detonation masking and schlieren effect. The procedure for the wet-wall test runs in the square test section was as follows:

1. Replace the driver diaphragm and evacuate the driver and test section.
2. Fill the test section with oxygen.
3. Remove the exhaust section and apply the DECH to the walls with oxygen flowing in the test section.

4. Replace the exhaust section.

5. Fill the driver with premixed hydrogen-oxygen.

6. Fire the spark plug in the driver section.

Two different methods of applying the liquid to the walls were used. First a known quantity of fuel was poured in from the top and allowed to run down the sides. Second, a felt swab which had been wetted with fuel was run up the tube wall to the 1.5 ft mark. In some of the tests only one wall was coated—the solid wall containing the pressure transducers. In other tests the two solid walls were coated.

Pressure and velocity results for the wet-wall tests are shown in Table 3 and typical pressure traces are shown in Fig. 11. For the case when DECH was swabbed on two walls the measured velocity was 3750 ft/sec and the pressure ratio was 17 to 1. When DECH was swabbed on one wall only the measured velocity was 3160 ft/sec and the pressure ratio was 10.5 to 1. In both cases the strength of the propagated wave is lower than the initial strength of the transmitted shock but at the end of the test section the propagated wave is much stronger than the transmitted shock into nitrogen, which indicates that a chemical reaction is driving the shock front. Framing camera photographs of these tests in Fig. 12 show that the reaction originates at the wall and spreads inward from the wall until about 250 μsec after passage of the initial front at which time the entire width of the channel is filled with luminosity. The more intense luminosity which extends across the channel starting with frames 9 and 22 in run 17 are the reflected waves off the exhaust diaphragm and the end of the exhaust section respectively. Additional combustion may be taking place across these reflected shocks but more information on the state of the gas is needed to ascertain this

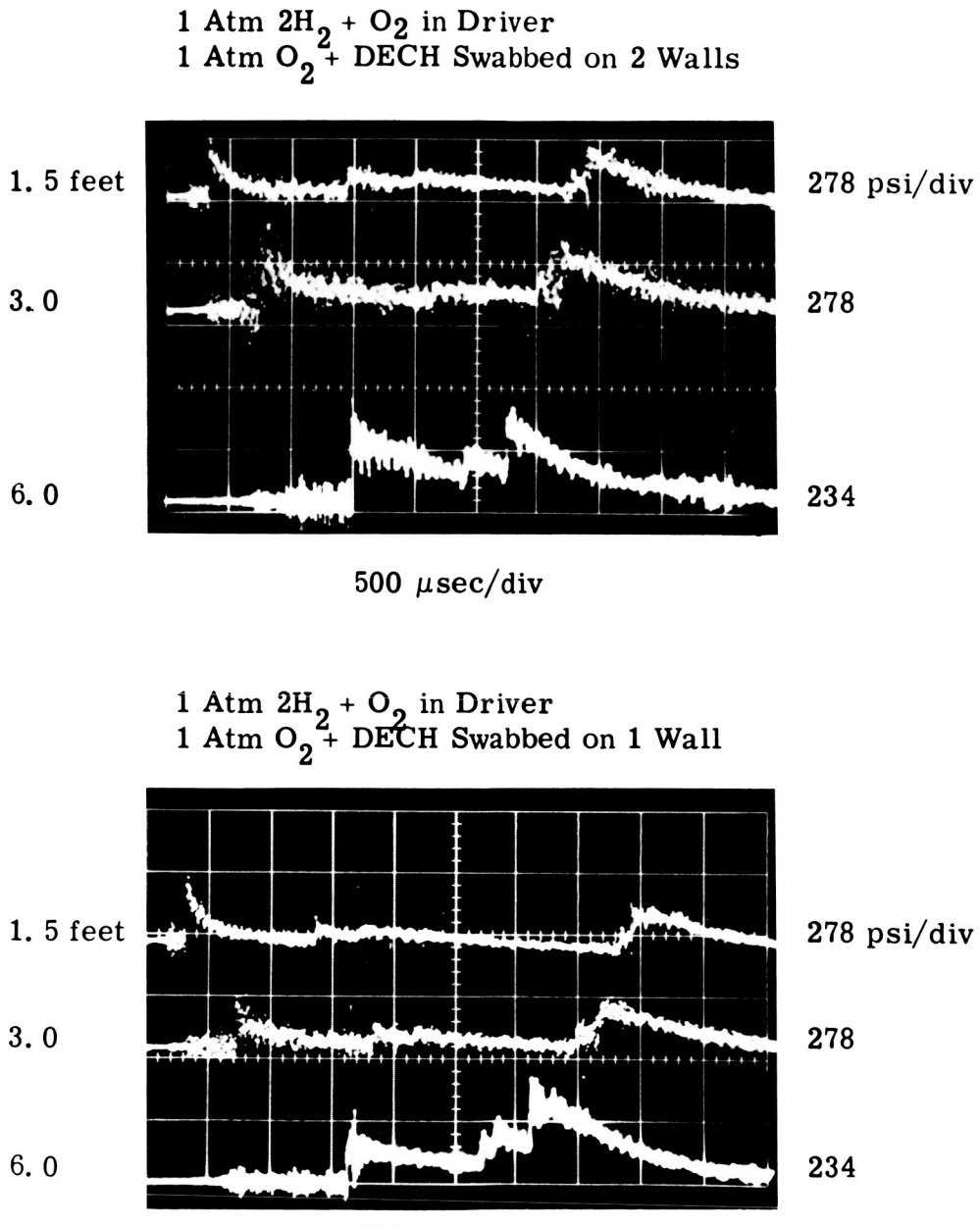

Figure 11. Pressure Traces of a Shock Reinforced by the Combustion of DECH Placed on the Walls of the Tube.

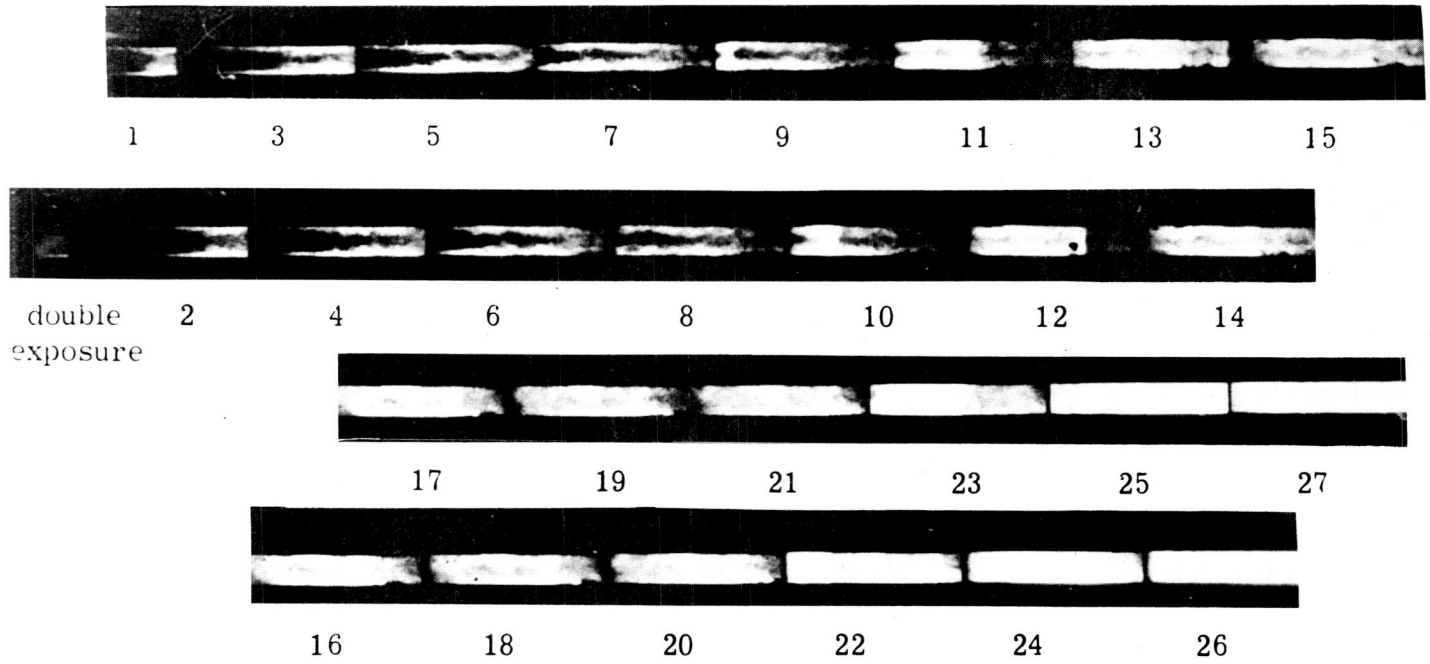

Run 17: 1 atm $2H_2 + O_2$ in driver; 1 atm O_2 + 12 ml DECH poured on two walls; 38.4 μsec between frames; initial wave moving from right to left.

Figure 12. Framing Camera Photographs of Shock Reinforced by the Combustion of DECH Placed on Two Walls of the Tube.

fact. In the case where only one wall has been wetted with fuel (Fig. 13) it appears that combustion zones are influenced more strongly by the initial shock structure. In particular, there are two zones of intense combustion, the second zone following the first by about 6 in. or 160 μsec. The distinct diagonal lines of luminosity which are present in frames 1, 2, and 3 of Fig. 13 indicate the possibility of oblique shocks which are caused by the heat release. By slightly damping the ringing of the pressure transducers (with the sacrifice of rise time) it might be possible to sense these oblique shocks if they are present. The reflected waves off the exhaust diaphragm and end of exhaust section which appear in the pressure trace of Fig. 11 do not show up in the framing camera photographs, although there is a general increase in luminosity starting at about frame 15.

The spark schlieren photographs which were taken give additional information on the structure of this phenomenon. Figure 14 shows the normal shock transmitted into nitrogen. The shock is moving from left to right. The disturbance behind the shock is due to internal stress in the glass except for the curved disturbance about 3/4 of a channel width upstream which is due to a small recess in the wall. Similar pictures of the shock propagating into nitrogen with DECH applied to the walls were taken but no noticeable difference from Fig. 14 could be detected with the present setup. Spark schlieren photographs of the case where DECH is applied to two walls with oxygen in the test section is shown in Fig. 15. In one run the shock front is slightly convex, in another slightly concave. The dense reaction zone extending from the wall is quite closely coupled to the shock. The turbulence in the center of the channel directly behind the shock front may be due to the

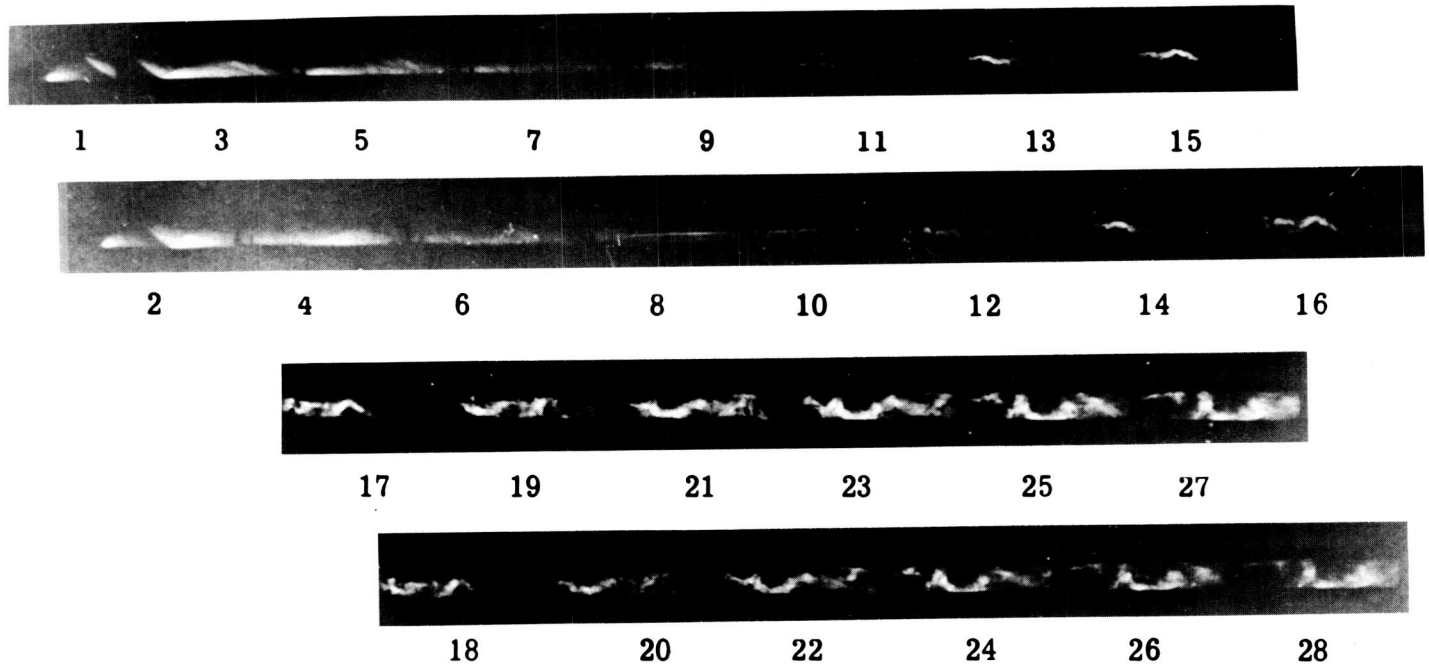

Run 21: 1 atm $2H_2 + O_2$ in driver; 1 atm O_2 + DECH swabbed on one wall (bottom of photos); 38.4 μsec between frames; initial wave moving from right to left.

Figure 13. Framing Camera Photographs of Shock Reinforced by the Combustion of DECH Placed on One Wall of the Tube.

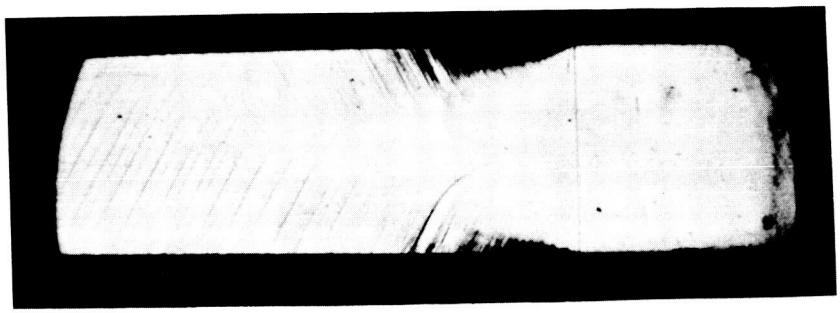

Figure 14. Spark Schlieren Photograph of a Normal Shock Propagated into Nitrogen.

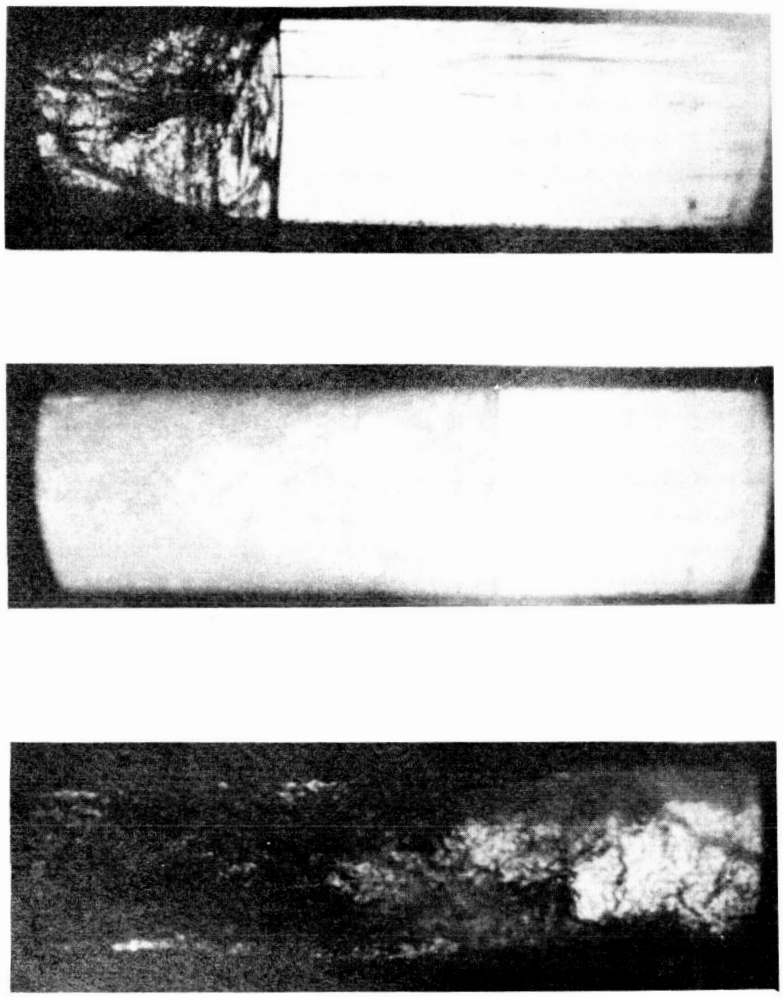

Figure 15. Spark Schlieren Photographs of a Shock Reinforced by the Combustion of DECH Placed on Two Walls of the Tube.

complexity of the shock front rather than chemical reaction. Spark schlieren photographs of the case where DECH is applied to one wall with oxygen in the test section are shown in Fig. 16. Here the reaction zone trails the leading shock system by 2/3 of a channel width or 30 μsec. The initial shock structure appears to be time unsteady. Since the schlieren mirrors were only six in. in diameter, the second intense combustion zone indicated in the self-luminous photographs does not appear. Theoretical and experimental work on this phenomenon are continuing.

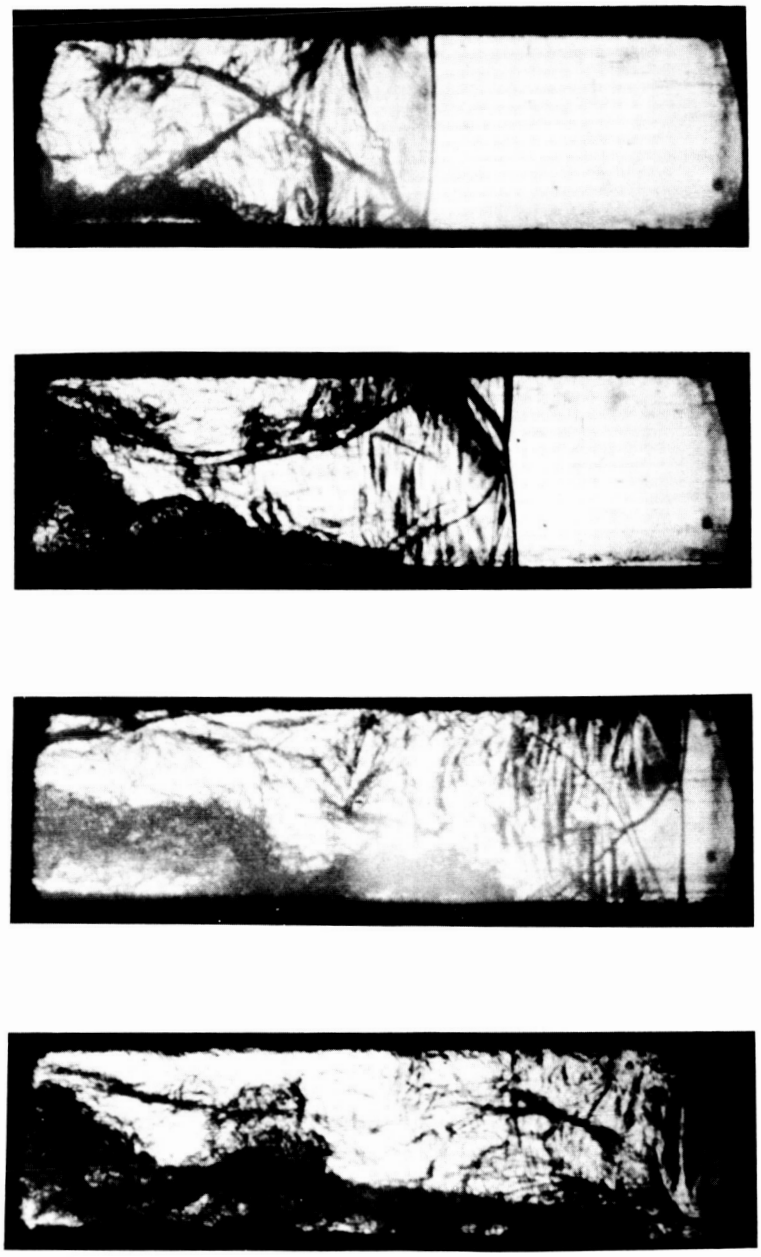

Figure 16. Spark Schlieren Photographs of a Shock Reinforced by the Combustion of DECH Placed on One Wall of the Tube.

III. PRODUCTION OF MONODISPERSE SPRAYS

As was mentioned earlier, the realization of a monodisperse spray would be important to the study of detonations in a two-phase system. Such a spray, if controllable would be very useful in that the effect of two important variables—namely drop size and overall fuel-oxidizer ratio—could be checked. The importance of these two parameters in deflagrative combustion has been shown experimentally by Burgoyne and Cohen[11], and the importance of the drop size in detonation has been theoretically predicted by Williams[2]. On this basis and on the basis of the fact that measurement of the drop size distribution in conventional sprays is subject to many sources of error as well as its being a tedious task[12-16], it was decided at the outset to investigate means of producing monodisperse sprays which can be precalibrated so that no size measurement would be required during testing.

A literature search showed that schemes for producing uniform size drops have been attempted in the past with apparently the most successful being that of Burgoyne and Cohen[17], which is based on the Sinclair-LaMer aerosol generator[18], and those of LaMer et al.[19] and Vonnegut and Neubaur[20]. The first two are based on the principle of condensation of a supersaturated gas and the latter on electrostatic atomization. In the first scheme, drop sizes of 7-50 μ were produced whereas in the latter schemes drops of the order of 1 μ or less were obtained. Since larger drops are also of interest to this study, it was decided to develop a new means of producing a field of uniform drops. It should be pointed out that recent experimental advances in producing single streams of uniform drops figured heavily in this

decision, for it was thought that producing a field would be a mere extension to such techniques.

Techniques for producing streams of uniform drops were developed by several investigators such as Dimmock[21, 22] (10-300 μ drops), Margarvey and Taylor[23] (500 μ - 20 mm), Mason et al.[24, 25] (30-1000 μ) who used vibrating capillaries, Raynor and Haliburton[26] (50-700 μ) whose device consisted of a rotating needle which scoops the same amount of water as it passes through a sheet of the liquid, and Wolf[27] (4-200 μ) who used a vibrating reed which impinges through the surface of water held in a slit cut through a piece of sintered glass. The drop size obtainable by the last two methods is very dependent on the penetration depth of the needle or reed. Furthermore, these methods are apparently limited to rather low frequencies (less than 150 cps). It was felt that extension of these devices such as by making use of multi-needles or reeds would prove difficult as well as inadequate. From a consideration of the requirement in a monodisperse system suitable to a detonation tube and the behavior of capillary jets, it will be seen that the vibrating capillary technique shows promise and therefore was chosen for development.

1. Required Properties of Monodisperse Systems

The best method to produce a monodisperse spray in a tube of a reasonable length as might be required for detonation studies appears to be that in which the tube is vertical with the drops generator at the top end producing drops at a steady rate which fall at their terminal velocity. Assuming such a generator is available the relationship between the number density of drops, the frequency of generation necessary, etc., and the drop size can be derived as follows.

Consider a drop of diameter D_ℓ falling at constant velocity in a gaseous atmosphere. Since the drag force must be balanced by the force due to gravity, we have:

$$C_D \frac{\rho_g u_\ell^2}{2} \cdot \frac{\pi}{4} D_\ell^2 = \frac{\pi}{6} D_\ell^3 (\rho_\ell - \rho_g) g \tag{16}$$

or, since $\rho_g \ll \rho_\ell$ usually,

$$D_\ell \cong \frac{3}{4} C_D \frac{\rho_g}{\rho_\ell} \frac{u_\ell^2}{g} \tag{16a}$$

Introducing the Reynolds number, we find

$$D_\ell^3 = \frac{3}{4} \cdot C_D \, Re^2 \left(\frac{\mu_g^2}{g \rho_g \rho_\ell} \right) \tag{17}$$

and

$$u_\ell^3 = \frac{4}{3} \frac{Re}{C_D} \left(\frac{\mu_g g \rho_\ell}{\rho_g^2} \right) \tag{18}$$

If the fuel is assumed to be in the liquid phase and the oxidizer in the gaseous phase the number density, N, can be derived to be

$$N = \frac{6}{\pi D_\ell^3} \left[\frac{\rho_g n \phi \frac{m_\ell}{m_g}}{\rho_\ell \left(1 - \frac{n \phi m_\ell}{m_g} \cdot \frac{\rho_g}{\rho_\ell} \right)} \right] \tag{19}$$

For most liquid hydrocarbons and for the fuel used in this investigation (DECH) the value of $n\,m_\ell/m_g$ is of the order of unity so that for mixtures at nearly stoichiometric proportion, Eq. (19) can be approximated to

$$N \cong \frac{6\rho_g n\phi m_\ell}{\pi D_\ell^3 \rho_\ell m_g} \tag{19a}$$

For uniform spacing between drops, the drop generator should produce drops at a number of points per unit area equal to $N^{2/3}$ and at a frequency

$$f = u_\ell N^{1/3} \tag{20}$$

It is of interest to know the rate of volumetric accumulation per unit area, Q, falling at the bottom of the tube:

$$Q = Nu_\ell \frac{\pi D_\ell^3}{6} \tag{21}$$

Considering a stoichiometric mixture of the fuel DECH with oxygen as the oxidizer at NTP, the relationship between D_ℓ and u_ℓ can be found from Eq. (17) and (18) as shown in Fig. 17. Also shown are the variations of N, f and Q with D_ℓ. For computation, the values of C_D and Re were taken from Schlichting[28] and

$\rho_g = 1.43 \times 10^{-3}$ gm/cm^3	oxygen
$\mu_g = 2 \times 10^{-4}$ poise	oxygen
$m_g = 32$ gm/mole	oxygen
$\rho_\ell = .8$ gm/cm^3	DECH
$m_\ell = 140$ gm/mole	DECH
$n = 1/15$	

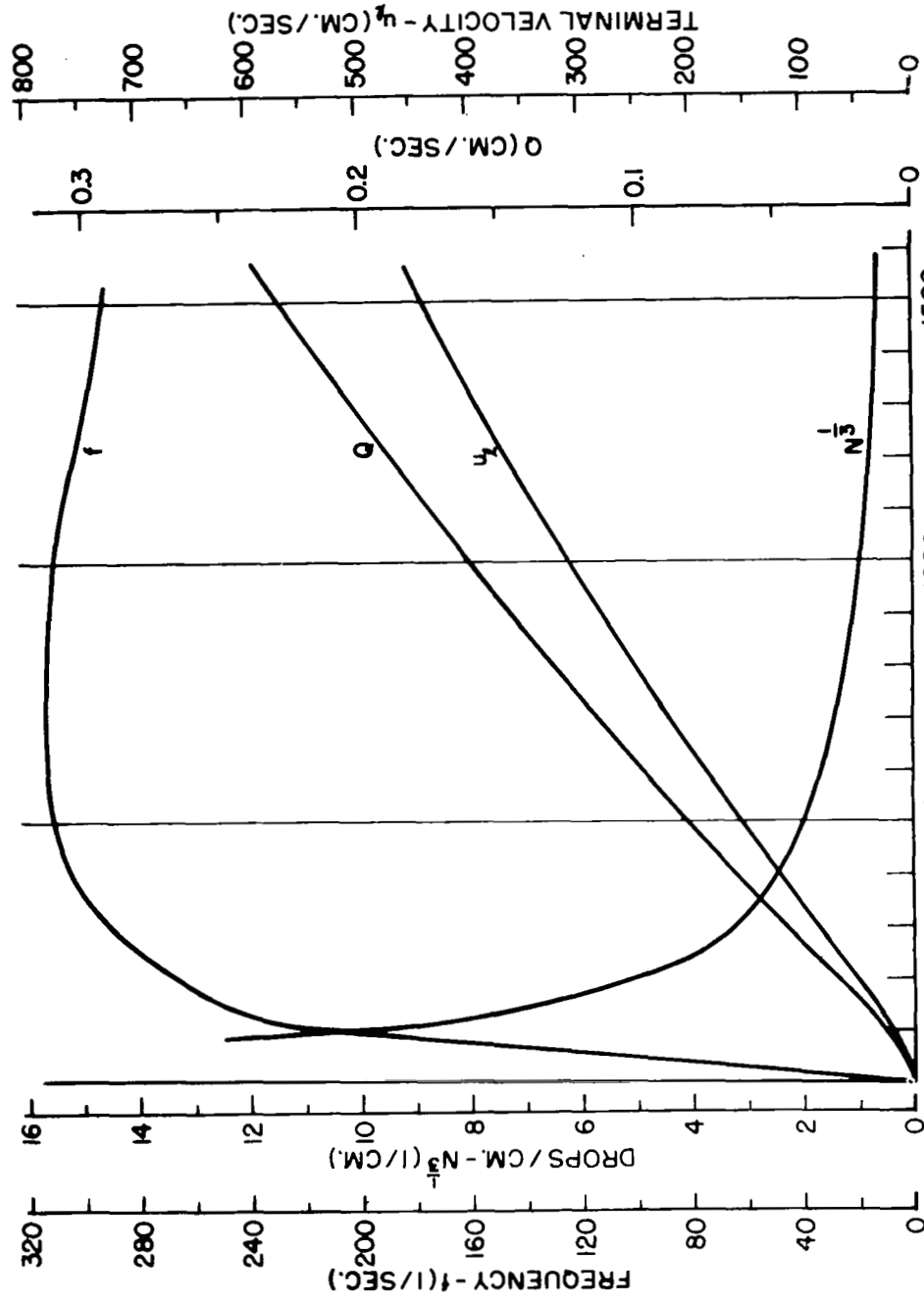

Figure 17. Terminal Velocity, Frequency, Number Density and Volumetric Accumulation as a Function of Drop Diameter for Stoichiometric DECH in O_2 at 1 Atmosphere.

were used. It is interesting to note that the frequency remains relatively constant in the drop size range of interest, namely 100-1000 μ.

2. Properties of Capillary Liquid Jets

All vibrating capillary devices for producing a stream of uniform drops are based on Rayleigh's analysis of the instability of capillary jets[29] which was made after the experimental observations of Savart[30] on the breakup of liquid jets. If the form of the perturbed cylindrical jet surface is described by

$$r_j = r_{j0} + \Delta r \cos \frac{2\pi}{\lambda} z \tag{22}$$

where $\Delta r / r_{j0} \ll 1$ and if

$$\Delta r = \Delta r_0 e^{qt} \tag{23}$$

Rayleigh shows by calculating the change in the potential energy and the kinetic energy from the unperturbed condition and using Lagrange's method that the amplification parameter, q, can be derived as:

$$q^2 = \frac{\sigma}{\rho r_j^3} \cdot \frac{(1 - x^2) \times I_1(x)}{I_0(x)} \tag{24}$$

where $x = 2\pi r_j / \lambda$. A plot of this equation in Fig. 18 shows that for the disturbance to amplify the wavelength should be greater than the jet circumference and that the amplification factor is maximum at $\lambda / d_j = 4.508$. If the jet velocity is u_j, then the frequency for maximum instability is

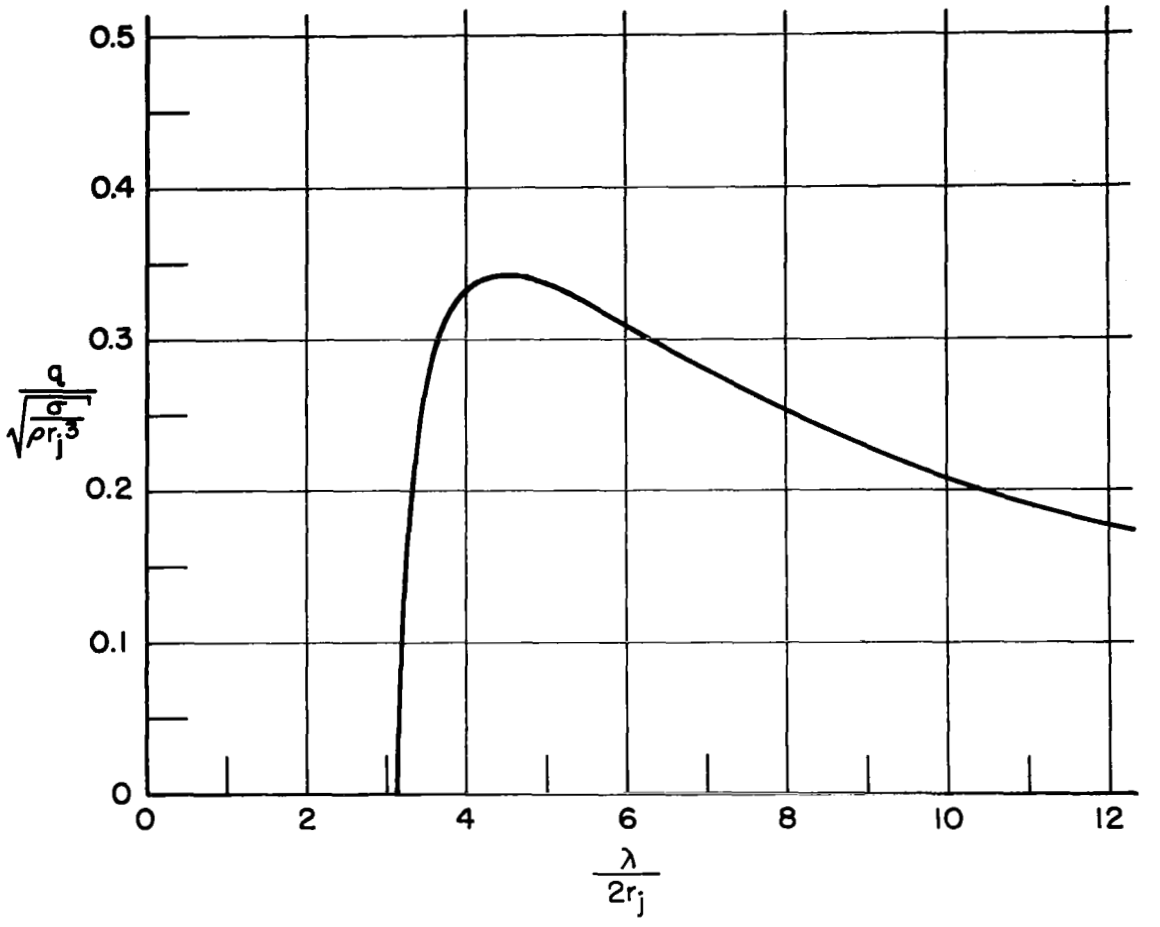

Figure 18. Capillary Jet Disturbance Amplification Parameter Variation with Wavelength to Diameter Ratio.

$$f = \frac{u_j}{4.508\, d_j} \tag{25}$$

When the jet is mechanically disturbed at such a frequency, drops of uniform size are formed. According to Schneider and Hendricks[31] however a range of frequency, such that $3.5\, d_j < \lambda < 7d_j$, can still result in uniform size drops. Of course the drop size will depend on the frequency as it can be easily shown from conservation of volume, that

$$\frac{D}{d_j} = \left(\frac{3}{2}\frac{\lambda}{d_j}\right)^{1/3} \tag{26}$$

where the drop volume is considered equivalent to that of a one wavelength long cylinder of the jet. It can also be shown that

$$\frac{\lambda}{D} = \left(\frac{2}{3}\frac{\lambda^2}{d_j^2}\right)^{1/3} \tag{27}$$

Equations (26) and (27) give $D/d_j = 1.89$ and $\lambda/D = 2.38$ at the frequency of maximum disturbance amplification.

It should be pointed out that Rayleigh's analysis is effectively applicable to a stationary capillary column of an inviscid liquid. Weber[32] extended the analysis to include the effects of the liquid viscosity, and the velocity of the jet. However Crane, et al.[33] show that if the velocity is low (less than 10 m/sec) these effects can be neglected.

When a liquid is forced through a small hole or a capillary tube, it is noticed that if the liquid head is small, the liquid forms a small drop which is attached to the exit surface by the action of surface

tension. The drop grows and when it reaches a size such that its weight can overcome the surface tension it detaches from the surface and falls. Drops formed this way are usually large. Now if the liquid head is increased, there is a pressure level at which a jet of a diameter equal to the exit diameter is formed. The jet usually disintegrates into irregular drops at a short distance away from the exit. However, if forced oscillations at frequencies compatible with Rayleigh's analysis are imposed on the exit plane, the drops become regular.

The minimum velocity of a smooth jet exiting from capillary tube is found by Schneider[34] to be dependent on the surface tension and the density of the liquid, and the diameter of the jet. His analysis is as follows. The flow inside the capillary is considered Poiseuille flow so that the velocity of the liquid in the tube is $u_t = f(r)$, and the velocity of the liquid in the jet, u_j, is considered constant across the jet. By considering a control volume near the exit plane an energy balance gives

$$\int_0^{r_t} \frac{\rho u_t^2}{2} 2\pi r \, dr \, u_t = 2\pi r_j \sigma u_j + \frac{\rho u_j^2}{2} \cdot \pi r_j^2 \cdot u_j \tag{28}$$

The first term on the right hand side is the rate of producing potential energy due to surface tension. For Poiseuille flow:

$$u_t = 2 \bar{u}_t \left[1 - \left(\frac{r}{r_t}\right)^2\right] \tag{29}$$

therefore Eq. (28) becomes after integrating:

$$\rho \bar{u}_t^3 r_t = 2 \sigma r_j u_j + \frac{1}{2} \rho u_j^3 r_j^2 \tag{30}$$

From continuity of mass this equation simplifies to

$$\bar{u}_t^2 = \frac{2\sigma}{r_j \rho} + \frac{1}{2} u_j^2 \tag{31}$$

If the coefficient of contraction is defined as

$$C = \frac{r_j^2}{r_t^2} \tag{32}$$

then continuity gives

$$\bar{u}_t = c u_j \tag{33}$$

so that from Eq. (30)

$$C = \left(\frac{1}{2 - \frac{4\sigma}{r_j \rho \bar{u}_t^2}} \right)^{1/2} \tag{34}$$

For a stable jet C must be ≤ 1 so that Eq. (34) shows

$$\bar{u}_t^2 \geq \frac{4\sigma}{r_j \rho} \tag{35}$$

This equation shows that a capillary jet must have a certain minimum velocity before it can be established. Another way of showing this is as follows. Consider a container with an orifice of radius, r_t at its bottom and let the pressure, p, at the orifice be just high enough to equalize the force due surface tension, i. e. ,

$$p \pi r_t^2 = 2 \pi r_t \sigma \tag{36}$$

For slightly higher pressure the liquid would start to flow and since for an incompressible flow the Bernoulli's equation gives

$$p = \frac{1}{2}\rho \bar{u}_t^2 \tag{37}$$

Eq. (35) can be obtained by combining Eq. (36) and (37). For low velocity jets satisfied by the equality in Eq. (35), C is unity and therefore $\bar{u}_t = u_j$ whereas for very high velocities, $C \to \sqrt{2}/2$. Schneider shows that Eq. (35) agrees very well with his experiments. Crane et al., (33) obtained for relatively high velocity water jets, a diameter contraction of ~ 80% or $C \cong .64$ which is in a reasonable agreement with the theory.

Since our work will deal mainly with relatively low velocities the jet diameter will be considered equal to the tube diameter. Some working plots are shown in Figs. 19, 20, and 21. Figure 19 shows the pressure drop for DECH at several tube diameters. On the same figure the minimum velocity calculated by Eq. (35) is also shown. The pressure drop was calculated assuming Poiseuille flow, so that:

$$\frac{\Delta p}{L} = \frac{32\,\mu u_t}{d_t^2} \tag{38}$$

For all tube sizes shown the Reynolds number at velocities near the minimum are below 2000, thus justifying the use of Poiseuille flow.

Figure 20 shows the frequency that would give maximum disturbance amplification when the jet velocity is at a minimum. This was obtained by combining Eq. (25) and (35) so that

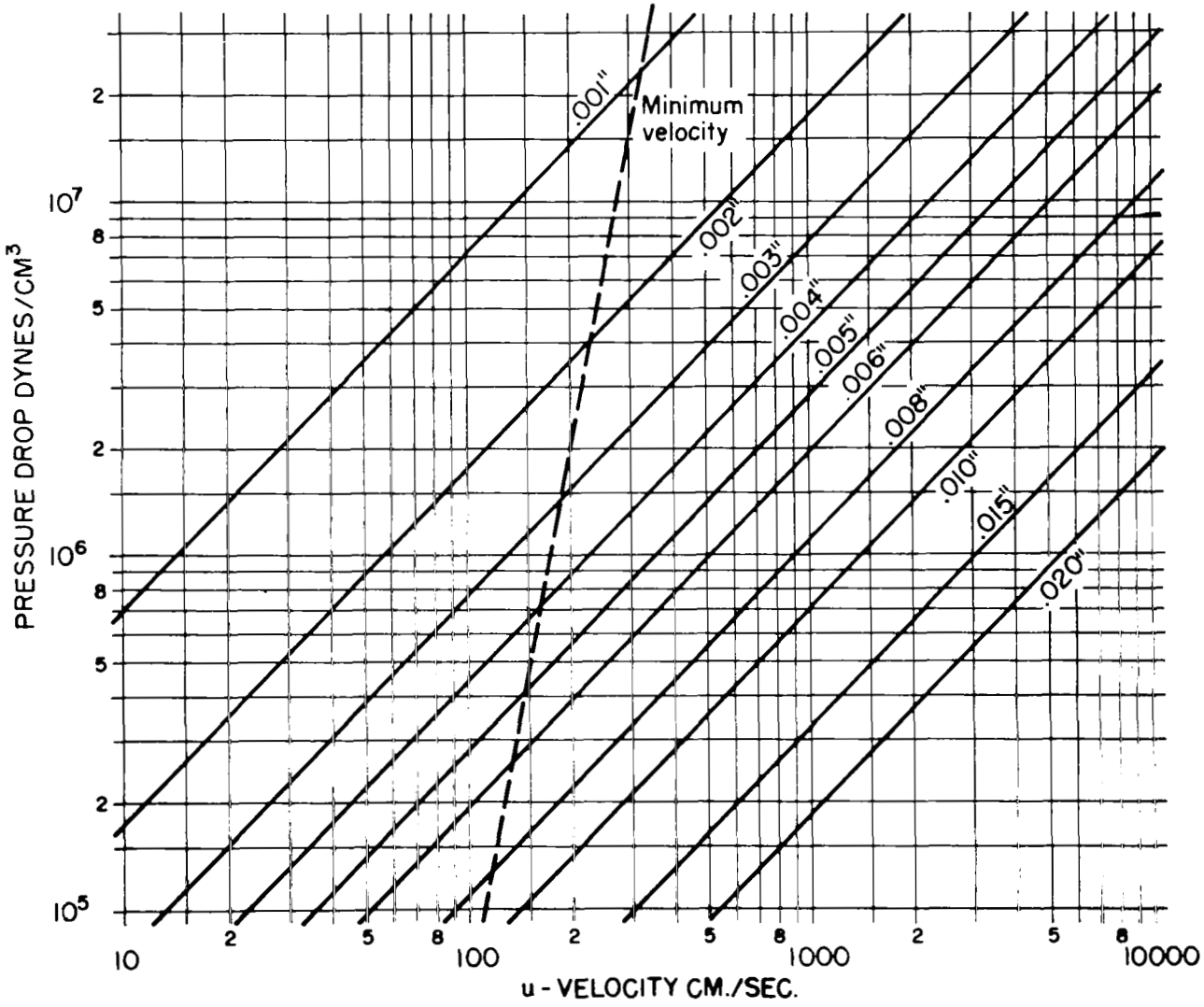

Figure 19. Pressure Drop Gradient in Capillary Tubes for DECH.

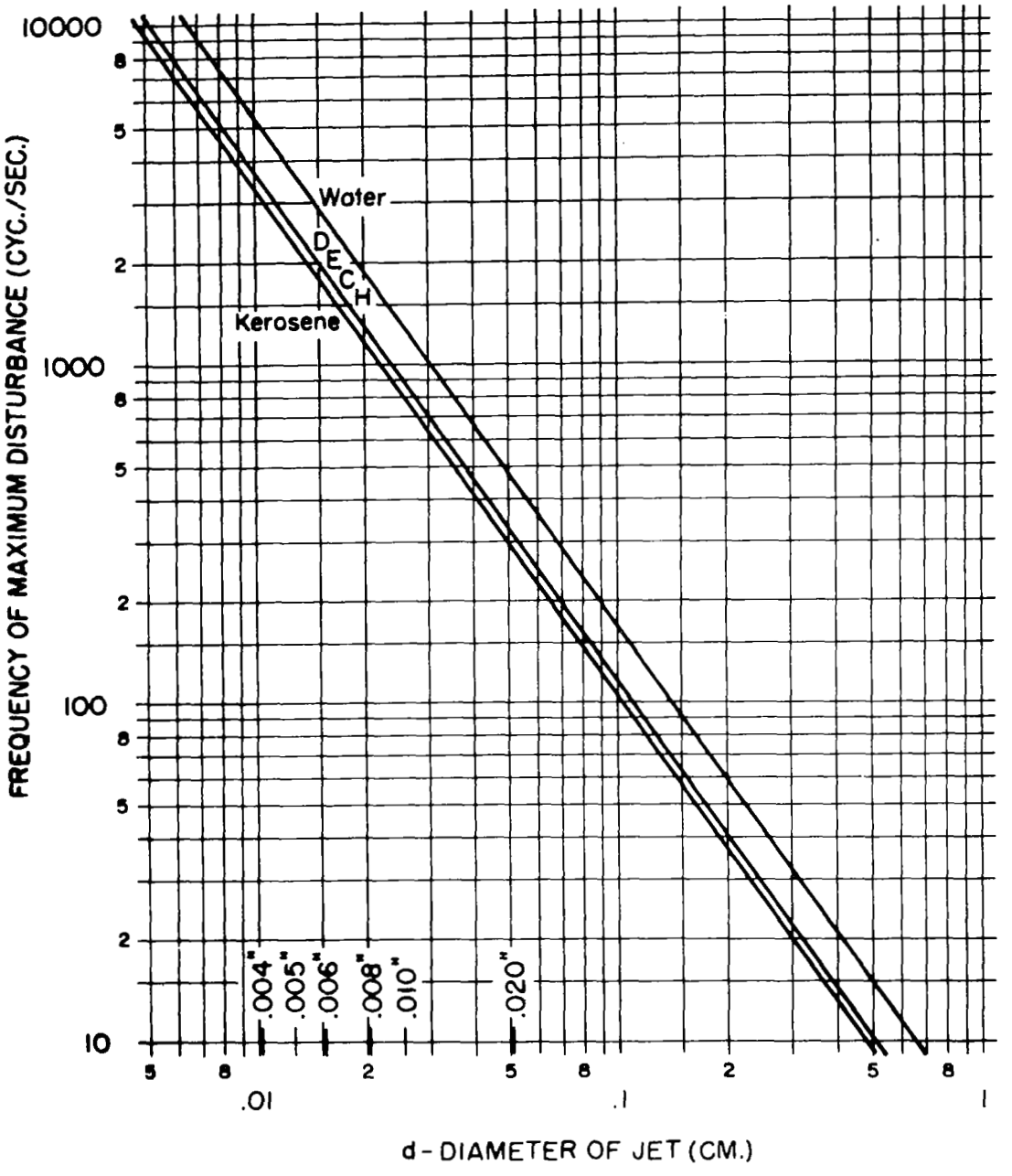

Figure 20. Frequency at Maximum Amplification Parameter for Water, DECH and Kerosene.

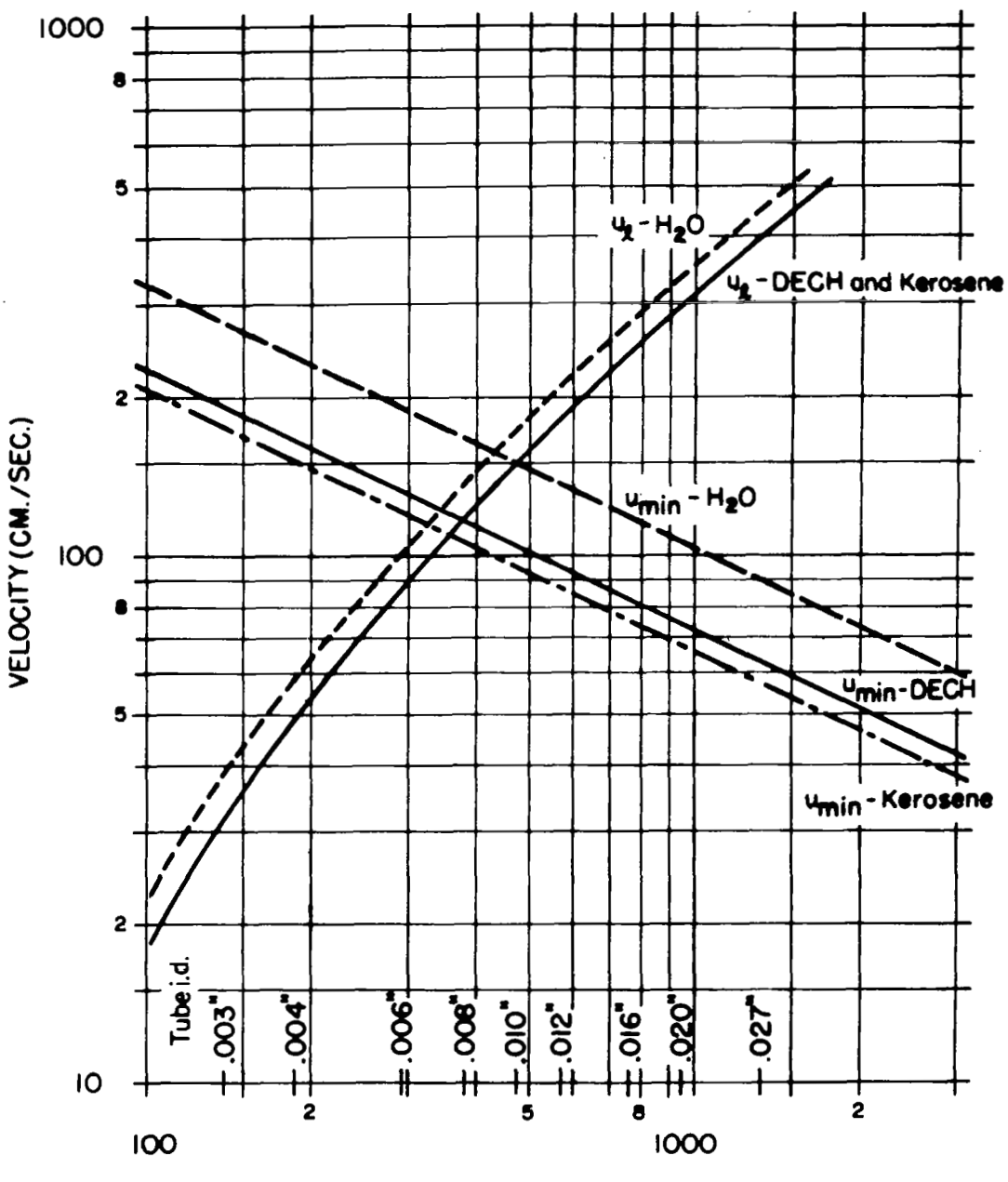

Figure 21. Terminal and Minimum Velocities of Drops in O_2 Atmosphere for Water, DECH and Kerosene.

$$f = 1.33 \left(\frac{\sigma}{\rho d_t^3} \right)^{1/2} \tag{39}$$

Figure 21 shows the terminal velocity of water, kerosene, and DECH drops falling in oxygen at NTP. On the same plot the minimum initial drop velocities—assumed equal to the minimum jet velocities—are shown. The drop size is found from Eq. (26) for the case of maximum disturbance amplification, and the minimum velocity is calculated by Eq. (35). It can be seen that for each liquid there is a certain size tube which would result in a terminal velocity equal to the minimum velocity. When larger tubes are used the terminal velocity is greater than the initial drop velocity so that the distance between drops increases as they fall. For smaller tubes the distance between drops tends to decrease which may result in collisions and coalescence. The coalescence problem will be discussed in the next section.

3. Drop Generator

After preliminary experimentation it became apparent that the best method for generating drops of uniform size for our purpose would be a modification of that of Margarvey and Taylor[23]. A schematic diagram of the system is shown in Fig. 22. The liquid is forced into the generator chamber which is vented to eliminate air bubbles. The generator chamber can be fitted with a plate having the desired number of capillary tubings of the desired size. Figure 23 shows the chamber fitted with a ten, gauge 30 needles spaced 0.25 cm apart. To insure uniform velocities of the issuing jets, needles of the same length were used. Needles of 0.63 cm length were precut by the manufacturer*

*Superior Tubing Company, Norristown, Pa.

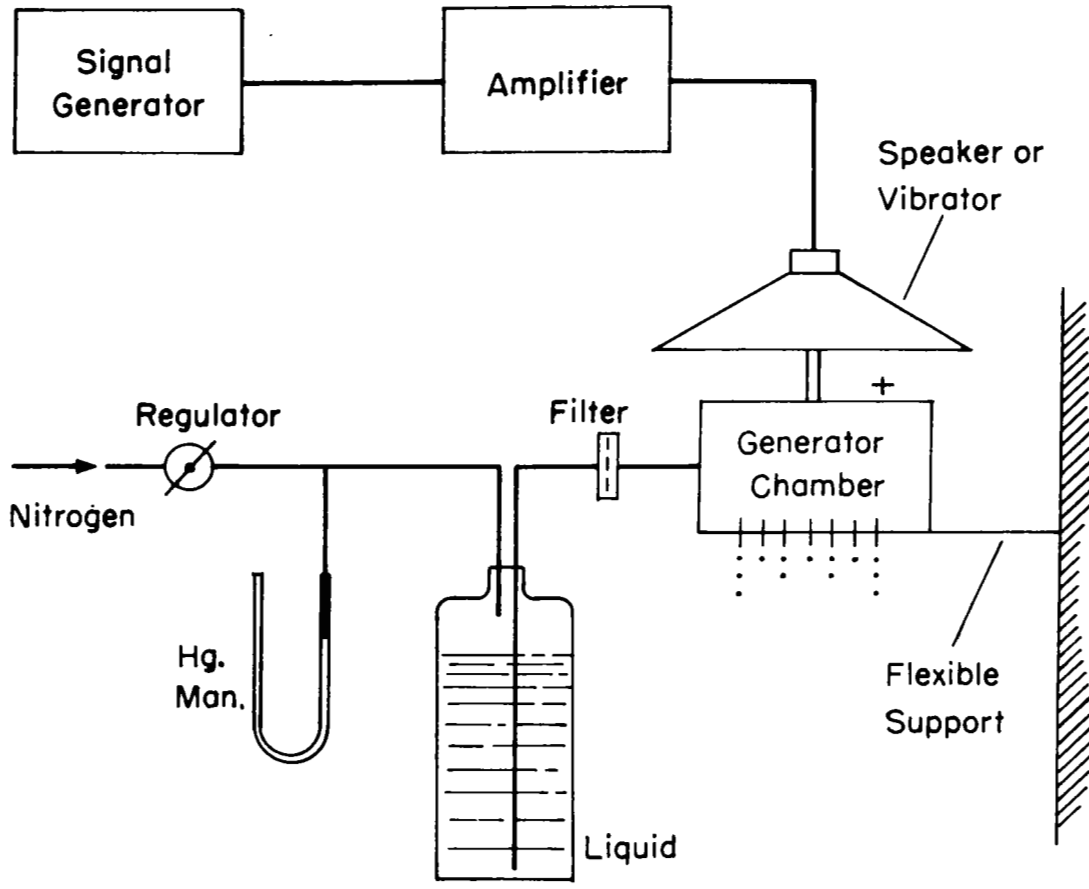

Figure 22. Schematic Diagram of Drop Generator.

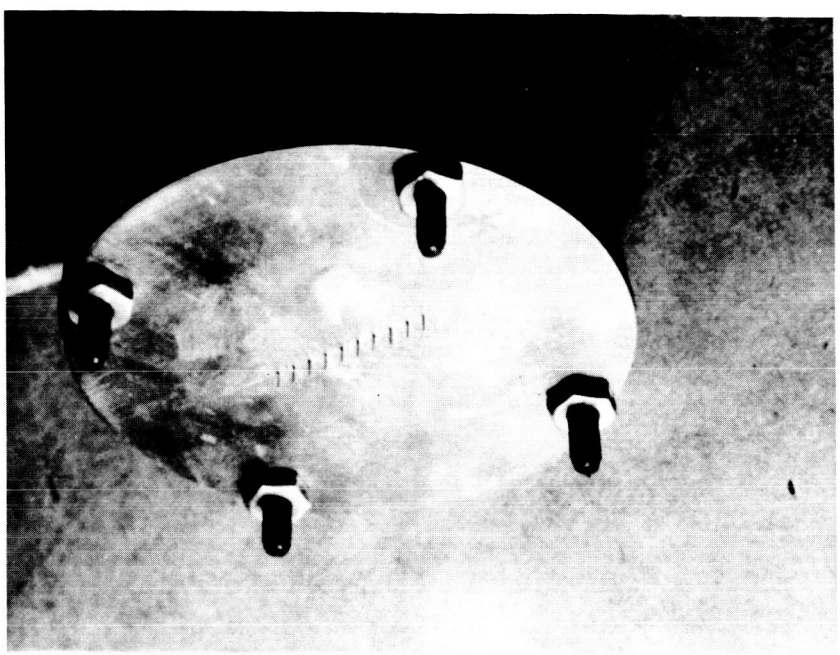

Figure 23. Drop Generator Chamber.

and were found to have clean and smooth ends. However, sometimes the needles did get clogged and the addition of an appropriate filter was helpful in reducing the problem. It was also found that one of the easiest ways of attaching the needles to the plate was first to mount and epoxy to the plate short pieces of tubes whose inside diameter is large enough to accommodate the needles. The latter were then inserted and epoxied. They were intentionally made longer than the plate thickness with protrusions from either of its side. The protrusions from the inside are helpful in eliminating the accummulation of any particles at the tube inlet that would result in clogging, whereas those from the outside were found helpful in eliminating any creeping of the liquid from the needles to the bottom plate surface which can cause dripping from the surface.

When the flow through the needles is established, the whole generator is vibrated by a speaker which is mechanically attached to it. The speaker is driven by a signal generator of variable frequency through an amplifier. For a drop generator smaller than the one shown in Fig. 23 the speaker was adequate. However for the large generator which weighs about 200 gms, a vibrator manufactured by the MB Manufacturing Co. Model C31 was used and is shown in Fig. 24. A proper selection of the frequency results in regular drop formation which can easily be observed by a stroboflash unit.

Most of our experimentation was done using gauge 30 needles (I. D. = .006 in.) and either distilled water or odorless kerosene. The latter was used because its surface tension and density are close to those of DECH. In early experiments in which the generator was driven at a frequency about three times lower than the frequency of maximum

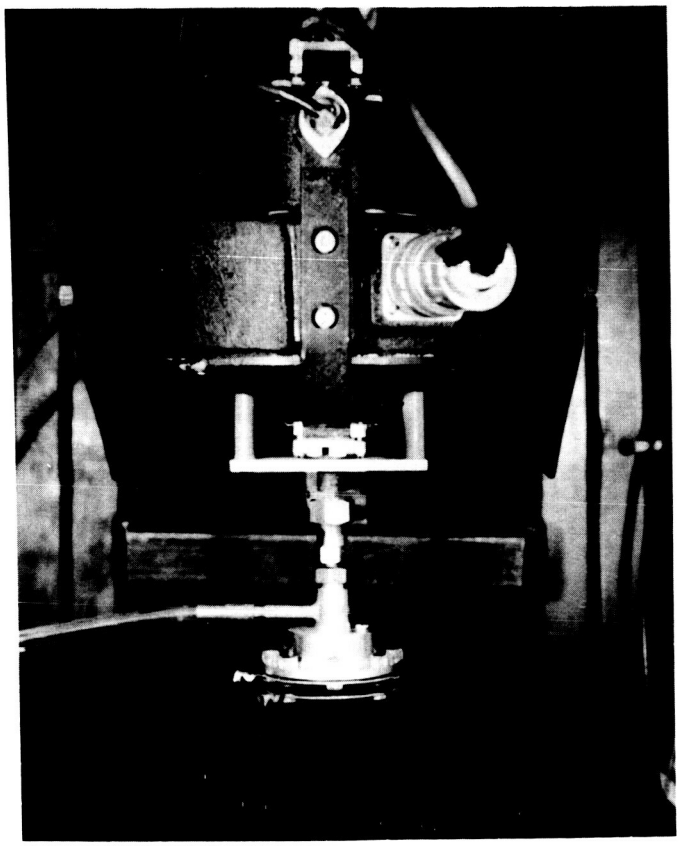

Figure 24. Vibrator and Drop Generator.

amplification, the drops generated were—as would be expected from Eq. (26)—large and initially evenly spaced. It was possible to obtain six streams with uniform size drops for about 15 cm of fall. It was noticed that thereafter the drops in one stream deviated from their mean position and started pairing off and eventually coalescence took place. Figure 25 shows a typical case in which pairing is evident in some streams and coalescence in others. In cases where the generator was driven at the frequency of maximum amplification, coalescence took place even earlier.

The encounter between two succeeding drops can be explained as follows. When the initial velocity of the drops is larger than the terminal velocity the drops must slow down due to the drag. Thus the spacing between succeeding drops diminishes making an encounter more likely. If the terminal velocity is much larger than the initial velocity the spacing between drops increases as they fall thereby eliminating collision. Figure 26 shows water drops generated by a 21 gauge needle resulting in about 1 mm diameter drop. The photograph was taken at 100 cm from the needle. As expected the spacing between drops did increase. However as can be seen from the photograph that even under these conditions pairing of some drops is taking place. The reason for this is believed to be the fact that the drops are actually following in the wake of the preceding ones. The result is that one drop travels faster because of the wake of its preceding one whereas the succeeding drop being now at a larger distance from its predecessor may not be affected by the wake and may travel at its normal velocity. Hence pairing can take place and the effect can be intensified until coalescence takes place. It is interesting to point out that the wake effect was recognized by Sweet[35] who developed a recording oscillograph

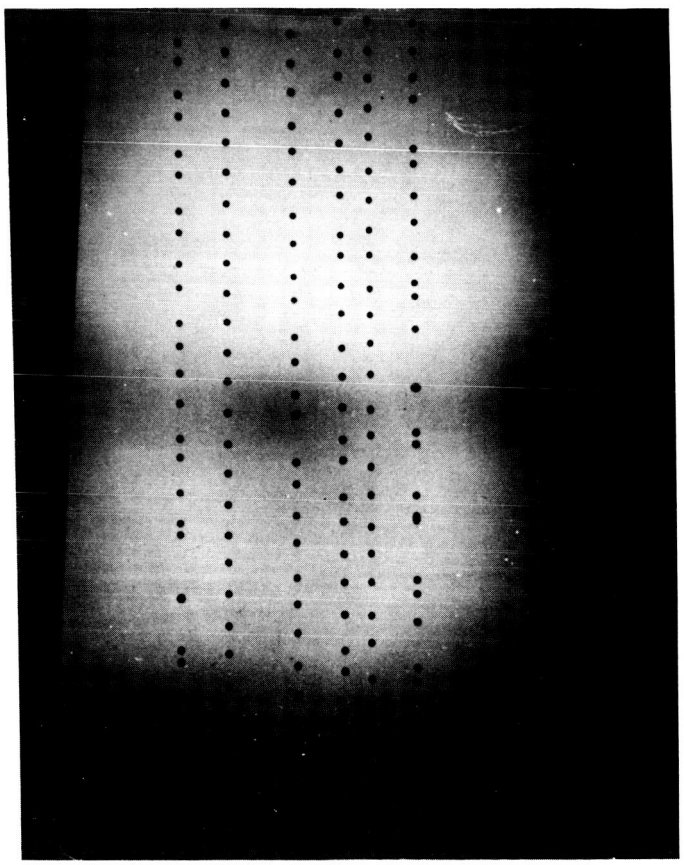

Figure 25. Six Streams Showing Pairing and Coalescence of Drops. (water, guage 30, f = 980 cps, 1 mm division on scale)

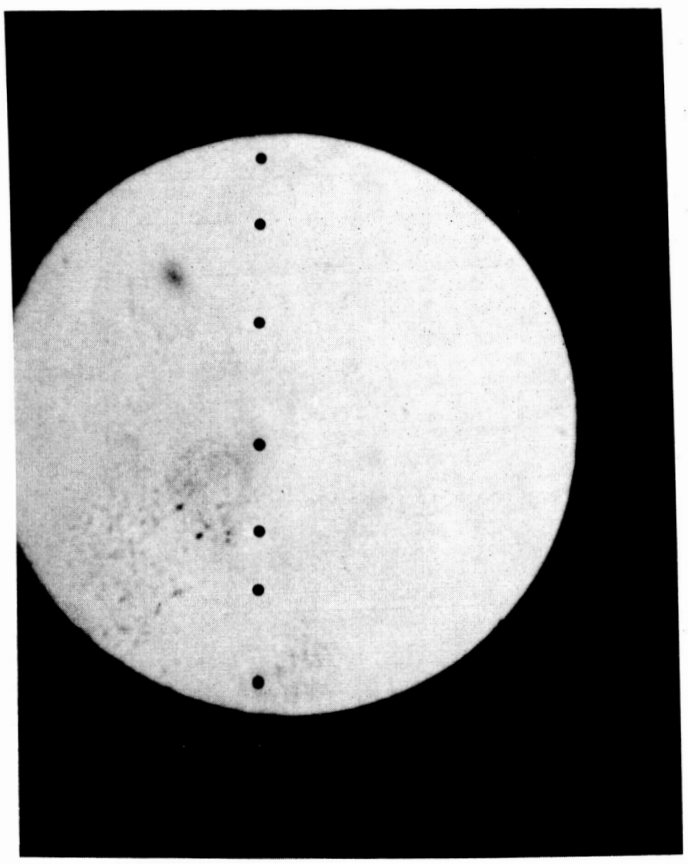

Figure 26. Drops Generated by Guage 21 Needle.
(water, 465 cps, image diameter = 5 cm)

which makes use of a vibrating capillary jet of ink. He found that distortion could be partially eliminated by blowing air transversely to the jet resulting in wakes at some angle to the drop stream rather than along the stream. Since in our case we were dealing with multi-streams the idea of side flows appeared impractical. Therefore other ideas were tried. However before we present these, the photographic system used will be described.

4. Photography of Drops

A single stream of drops can easily be photographed by backlighting it through a diffusing glass or screen. Since a magnified picture is usually required, the depth of focus is very limited. Thus if one needed to measure the sizes of drops in a spray, a tedious procedure requiring focusing at several planes in the spray is necessary. Bredfeldt[36] showed that the depth of focus can be increased appreciably by using collimated light behind the drops. The depth of focus, Δs, of a photographic lens can be written as:

$$\Delta s = \frac{2\left(\frac{f_1}{a}\right)(1 + M)\left(\frac{\Delta I}{I}\right) I}{M\left[1 - \left(\frac{\Delta I}{f_1}\right)^2 \left(\frac{f_1}{a}\right)^2\right]} \tag{40}$$

where f_1 is the focal length of the lens, a its aperture, M the magnification, $\Delta I/I$ is the tolerable fractional error when the object is off the focal plane, and I is the object size. When a collimated light produced by a source of a finite diameter d_s and a collimating lens of focal length f_c is used, the effective aperture ratio becomes f_c/d_s instead of f_1/a. So that Eq. (40) changes to:

$$\Delta s = \frac{2\left(\frac{f_c}{d_s}\right)(1 + M)\left(\frac{\Delta I}{I}\right) I}{M\left[1 - \left(\frac{\Delta I}{f_1}\right)^2 \left(\frac{f_c}{d_s}\right)^2\right]} \qquad (41)$$

The arrangement used in this study for photographing several streams of drops is shown in Fig. 27. The spark source operates through the discharge of six .02 μf capacitors charged at 20 KV. Its effective diameter is 1.6 mm and its duration is about 2 μsec. The collimating lens has a 7.5 cm diameter and a focal length of 35 cm, and the focusing lens diameter is 5 cm and its focal length 20 cm. Assuming a magnification of 1.5 and $\Delta I/I = .25$ for an object of dimension .015 cm, Eq. (40) shows that the depth of field is .05 cm whereas Eq. (41) shows Δs to be 2.74 cm. Thus a great improvement in the depth of focus is obtained when a collimated light is used. To illustrate this, calibrating wires were photographed using the two methods. Figure 28a shows the wires through diffused light whereas Fig. 28b through collimated light. The right hand vertical wire is .015 cm in diameter and all the others are .030 cm in diameter. The wires are held in a plane inclined 45° with the photographic axis so that the top horizontal wire is higher and behind the center wire by the same distance of 1.27 cm whereas the lower wire is below and ahead of the center wire by the same distance. The vertical wires which are really inclined 45° can be used to measure the depth of focus for any chosen $\Delta I/I$.

5. Status of Drop Generator

It is apparent from Fig. 17 and 20 that in general the frequency required to produce a stoichiometric mixture of DECH in oxygen does

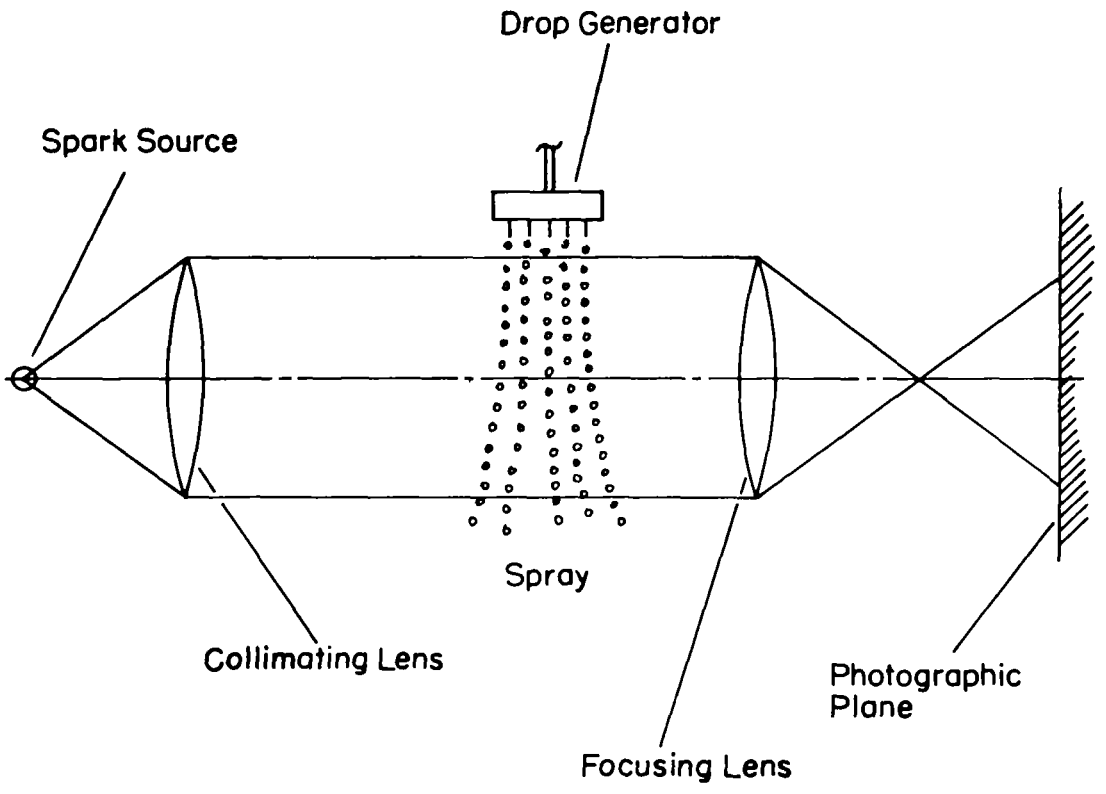

Figure 27. Photographic Arrangement of Sprays.

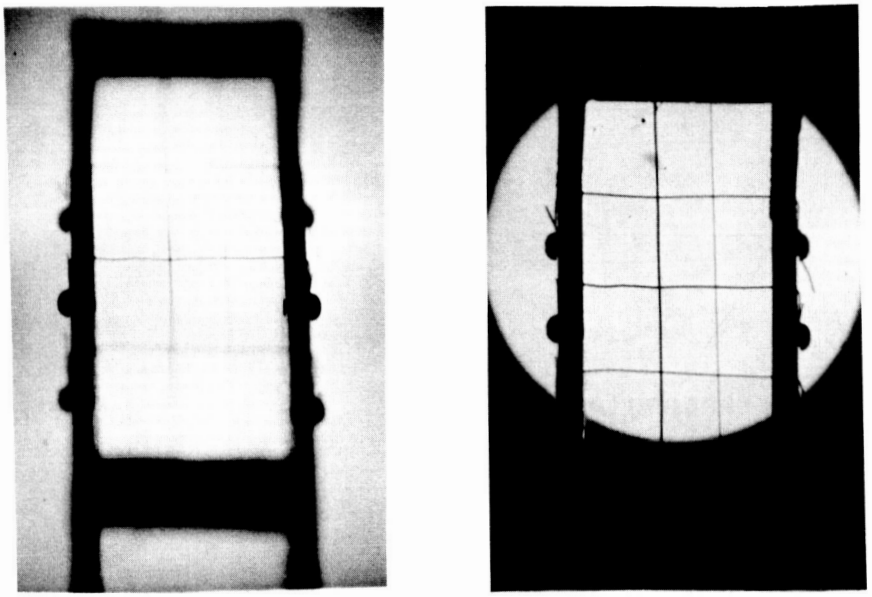

a) Through Diffused Light b) Through Collimated Light

Figure 28. Calibration Wires (. 3 and . 15 mm)

not correspond to the frequency dictated by Rayleigh's instability analysis. For example for a 284 μ diameter drop (as might be obtained by a .015 cm diameter jet), the frequency required is 287 cps whereas the frequency at maximum disturbance growth is 1950 cps. Inasmuch as the latter frequency is dictated by the physical properties of the liquid, there are only two approaches which can be followed to keep the number density as required. The first is to alter the number of generating jets by the ratio of the frequencies and the second is the removal of the excess drops generated. For the latter approach and for the above example about 6 out of 7 drops would have to be removed. A combination of these approaches is also possible; however, they are examined separately.

Effecting the first approach would be simple if it were not for the fact that coalescence has to be prevented. One way to do this is to electrically charge the drops as they form from the continuous jet. This method was tried with water. The drop generator is the same as that shown in Fig. 23 except the 10 needles were placed on 1.5 cm diameter circle. In addition a brass plate .16 cm thick which has ten 0.28 cm holes located so that they are concentric with the needles is placed at about .12 cm away from the tip of the needles. This charging plate is insulated from the needles and is held at a different potential from them by a D.C. power supply. Each jet and its corresponding hole in the plate form two elements of a condenser so that an electric charge is induced in the jet. As the drops form they carry this charge. The principle involved in this manner of charging the drops was used by Schneider[31] and Sweet[35].

Figure 29a shows a photograph of ten streams of uncharged drops formed by .015 cm I.D. needles. Because of the increased depth of

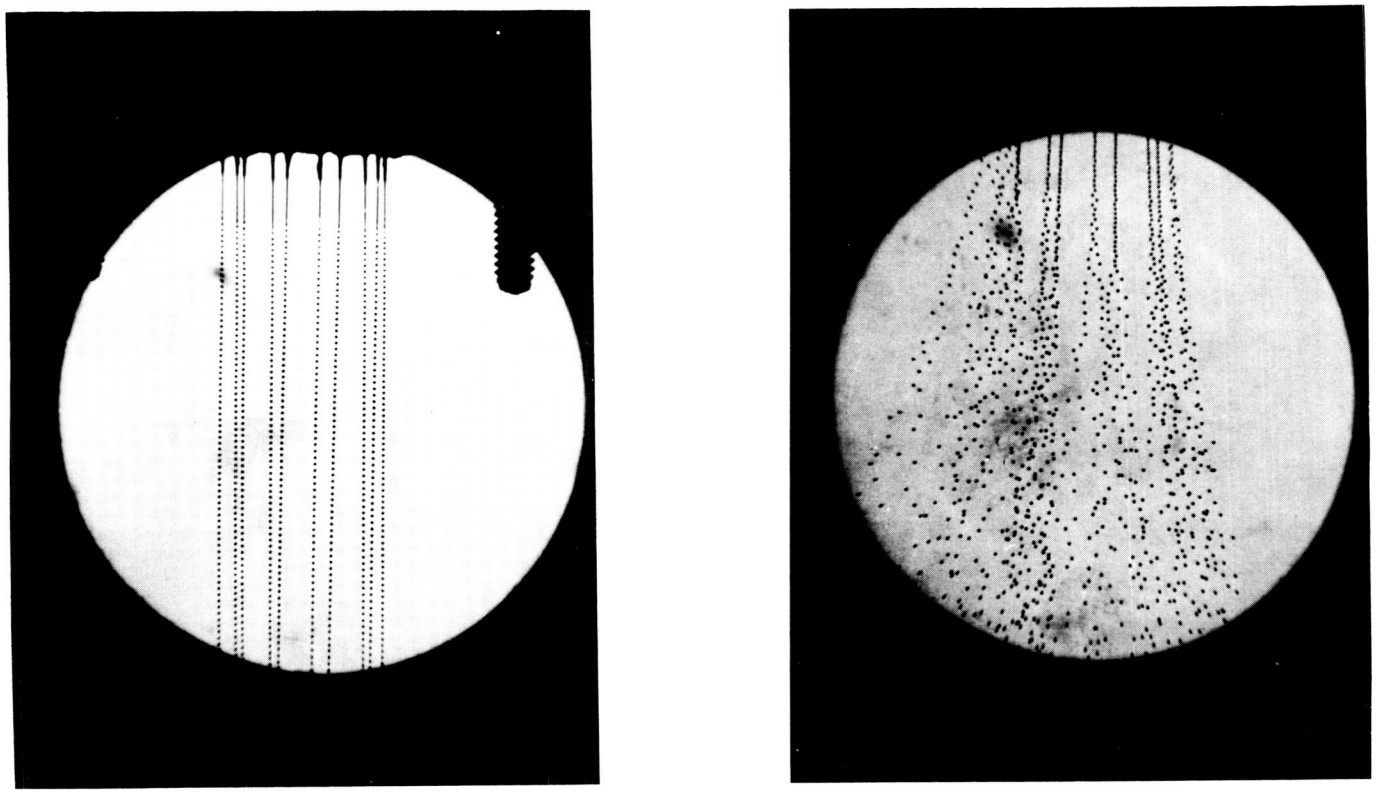

a) No Charge

b) With Charge 235 v.

Figure 29. Drops Generated by 10, Number 30 Guage Needles. (water, f = 2970 cps)

focus by use of a collimated light all streams appear in good focus. Figure 29b shows the effect of electric charge near the needles. It was found that in order to prevent any coalescence the voltage used must be high enough that a lateral motion of the drops takes place at a distance from the needle tip shorter than that at which coalescence starts in the absence of charging. Visual observation with a stroboflash indicated that no coalescence was taking place at a 2 meter distance from the needles. However, a disadvantage of this approach is that the spray continues to diverge due to the mutual repulsive forces between drops and hence the number density becomes variable. Although such a system may prove useful for other applications it is not suitable for the purposes herein.

To avoid this spreading out of the spray, opposite charges were induced in alternate streams. This was effected by using a charging plate made of plexiglass in which the holes were lined with a conducting material. Five alternating holes were connected to the positive side of a D. C. power supply and the other five were connected to the negative of a similar power supply. The negative of the first and the positive of the second were connected to the needles. The idea behind this technique is that the sprayas a whole has no net charge. Further the fact that two adjacent streams are separated by a distance much larger than that between drops of the same stream results in attractive forces much weaker than repulsive forces initially and therefore the probability of coalescence of drops from adjacent streams is small. However one would expect that some coalescence would eventually take place. Figure 30a shows how the spray appears initially when this technique is used. It will be noticed that little divergence takes place and that all drops are the same size indicating the absence of coalescence.

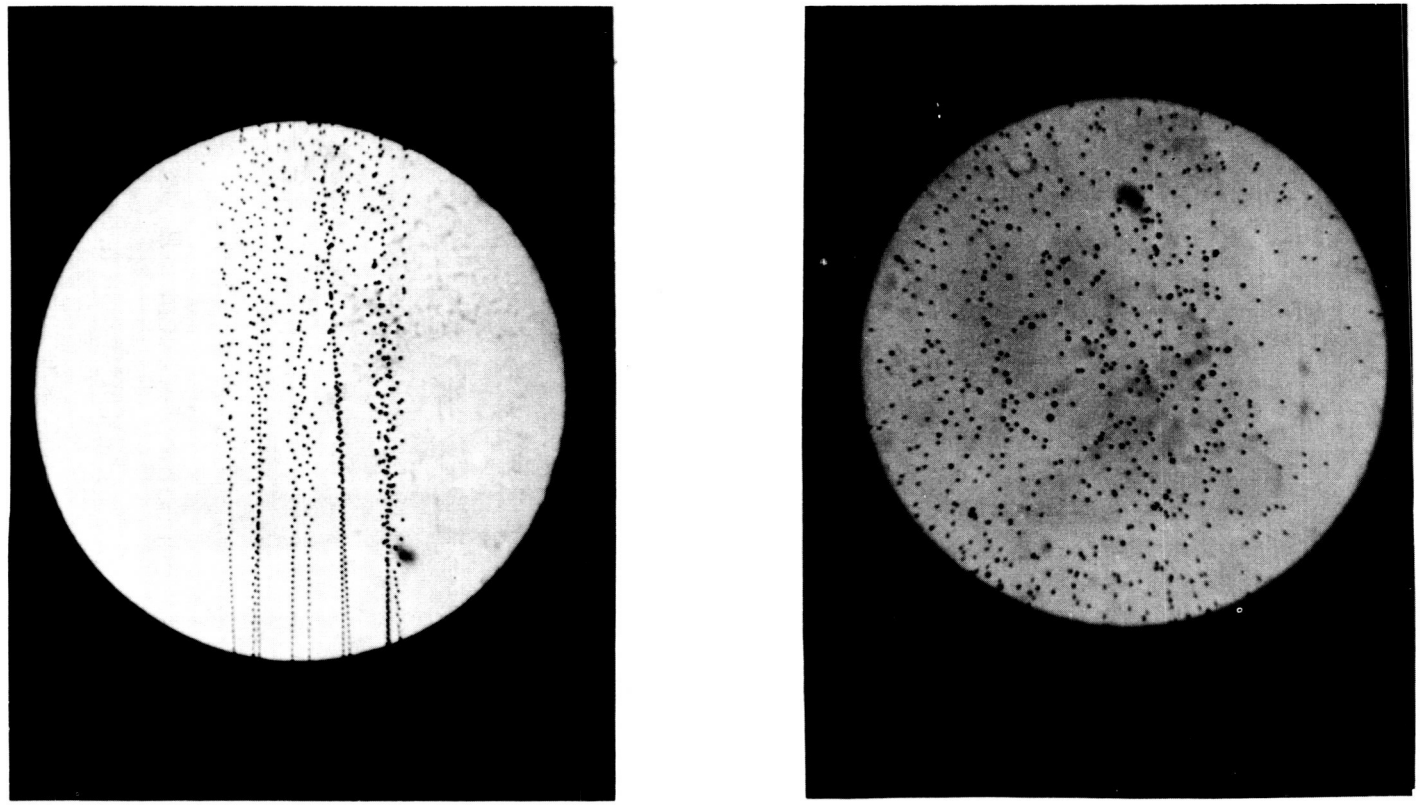

a) Close to Needles

b) 1 Meter Below Needles

Figure 30. Drop Generated by 10 Number 30 Needles With Alternate Charge. (water, f = 2970 cps $\pm$ 400 v.)

However at a distance of one meter below the needles, the spray exhibits divergence and coalescence as can be seen from Fig. 30b. The coalescence is found to be not as frequent as it would be if the streams were left uncharged and the divergence is not as much as it would be if all streams were charged with similar polarity charges. At present this technique is considered acceptable but still falls short of the ideal requirement.

The second approach which involves the removal of excess drops can be effected as follows. If the needles are located again on a circle and if the charging voltage is impressed periodically for a certain period of time corresponding to the formation of several drops and cut off for a period of time corresponding to one drop formation, then the charged drops would repel each other and move outwards whereas the uncharged drops would be unaffected and therefore keep on moving vertically. The charged drops can easily be interceded by a deflector whereas the uncharged drops are unimpeded. The principle of periodic charging can best be illustrated by two streams as shown in Fig. 31. Here the frequency of drop generation is 2800 cps and the frequency of a step charging voltage is 400 cps. The no-charge time was 1/7 the period. Thus one drop out of seven is expected to be uncharged. Unfortunately it appears that this scheme results in the coalescence of three drops as the photograph shows. Similar results were obtained with the ten needle generator. It is suspected that synchronization and phasing of the two frequencies are important. Sweet[35] used a somewhat similar principle on a single jet passing through an electric field and apparently was successful in avoiding coalescence. Instrumentation similar to his for synchronization and phasing will be used to perfect the system.

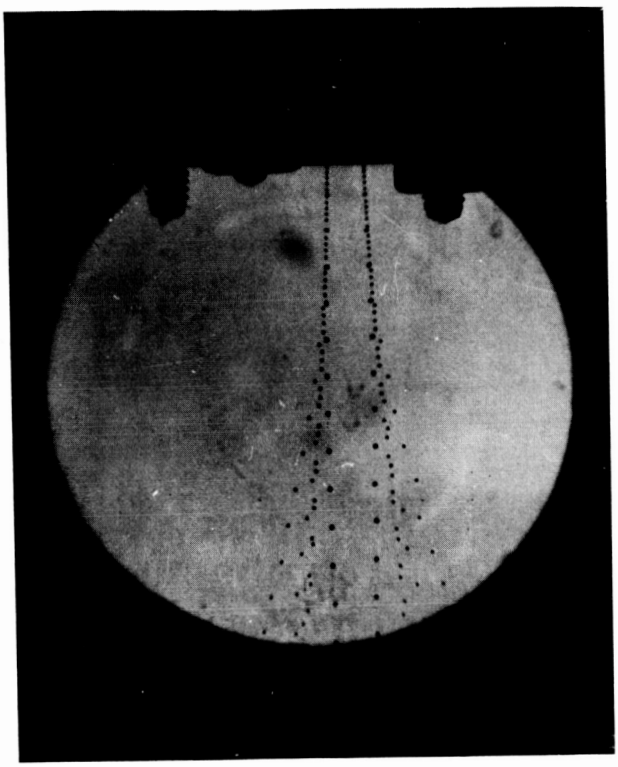

Figure 31. Drops Generated by Two Number 30 Needles, With Every Seventh Drop Uncharged.
(water, f = 2800 cps, charge - 400 v.)

All of the above experiments were made with distilled water. In any system that makes use of electrostatic charging the fluid resistivity is important as it affects the charging time constant[35]. Water has a resistivity of several orders of magnitude lower than hydrocarbons and therefore is relatively easy to charge so that when the latter are used it will be necessary to decrease their resistivity. Luther[37] used Shell ASA-3 antistatic additive to effect such a decrease in heating oil. Thus a similar technique will have to be used for DECH.

Before finalizing the drop generator design two other techniques will be tried to assess their merit. In the first air or oxygen flowing colinearly with the liquid will be used. This would accelerate the drops and therefore increase the distance between drops as they fall down. Hopefully this will prevent coalescence. The second technique will make use of a variable velocity gas flowing radially inwards at first and ending up axially downward. The idea behind this is to force successive drops into different trajectories and thus circumvent the wake effect.

IV. DROP SHATTERING

It has been shown in some preliminary droplet breakup experiments described by Nicholls and Cullen[38] that the strong shock wave associated with a detonation front is apparently capable of shattering droplets in a time sufficiently short that a detonation in a heterogeneous medium can become possible. However, due to the preliminary nature of these experiments, a more thorough investigation is required to rigorously establish the dependence of the breakup time and of the mechanism of fragmentation on the parameters of the problem. From the previous droplet breakup work of Engel[39], Hanson et al.[40, 41], and others summarized in Ref. (38) and the liquid jets breakup work of Morrell and Povinelli[42], the significant parameters appear to be the drop or jet diameter, the velocity, density, and viscosity of the gaseous medium, and the surface tension, density, and viscosity of the liquid with the dimensionless parameters being the Reynolds and Weber numbers. It is noteworthy, however, that these are the important variables for studies in which the maximum gas flow velocity encountered by the droplets never exceeds 10^3 ft/sec and the breakup times are of the order of milliseconds. Since the convective flow velocity behind a shock wave associated with a detonation front can be of the order of 5×10^3 ft/sec, it would be logical to extrapolate the results of the above authors. However, such an extrapolation can lead to erroneous inferences since, as pointed out by Engel[39], it is apparent that not only the rate of fragmentation but also the very mechanism by which it occurs is strongly dependent on the values of the test variables. It may therefore be suggested at this point that a third non-dimensional parameter, namely

the Mach number of the gas flow relative to the drop, is also important. This parameter is suggested because of its well known effect on the drag coefficient as the flow changes from a subsonic to a supersonic regime.

In an attempt to satisfy the requirements for an experimental investigation of the interaction between strong shock waves and liquid droplets which is considered pertinent to two-phase detonation, a shock tube has been designed in which the effects of the various test variables on the shattering phenomenon can be observed. The velocity of the gas flow can be controlled within a small range of variation through regulation of the shock Mach number, and the droplet generating mechanism can be easily adjusted to produce a variety of droplet sizes from fluids having a wide range of physical properties. Since it is apparent from the work of Rabin et al.[8] that the influence on the breakup process, when it is close to the critical pressure of the liquid, the design of the tube was made flexible enough that the pressure level in the test section could be varied also.

1. Description of Experimental Equipment

Initially it was felt that a combustion driven shock tube would be desirable for producing the strong shock waves required for the experiments. Since the shock Mach number increases monotonically with both the sound speed ratio and the pressure ratio across the diaphragm, the combustion driver provides increased shock strength through the effect of the heating process on both the pressure and the sound speed of the gas in the driver. After further consideration, however, it was decided to abandon the idea of combustion driving and to achieve the desired shock strengths by increasing the pressure ratio and using hydrogen as the driver gas. Rejection of the combustion driven technique was

based primarily on the fact that the reproducibility of specific experimental test conditions would be extremely difficult to achieve. Even though great care could be exercised in controlling the mixture ratio of combustibles and the initial pressure in the driver, the nonuniformities of the ignition process and of the combustion process are elements of each test over which there could be only limited control. Another experimental complication which has been attributed to the combustion process is that of irregularity in the flow field properties behind the shock wave. Byron[44] noted these effects in interferograms of the flow behind shock waves produced in a combustion driven shock tube. Needless to say that the occurrence of any flow field nonuniformities would add other unknowns to the list of variables in the droplet breakup problem, and therefore would complicate the interpretation of the experimental data.

The final design of the shock tube is shown in Fig. 32. It incorporates the use of a double diaphragm section — shown in Fig. 33 — between the driver and driven sections. The use of two diaphragms provides the operator with a simple means of controlling both the time at which firing of the shock tube is desired and the pressure ratio at the instant of diaphragm burst. The double diaphragm holder section consists of two rings placed between the flanges of the driver and the driven sections. To operate the tube, the desired pressure p_4 in the driver section is established simultaneously with the pressure p_D between the diaphragms ($p_D \simeq 1/2\ p_4$). The diaphragms are designed to break at a pressure differential in excess of $1/2\ p_4$, so that a reduction in p_D will fire the tube.

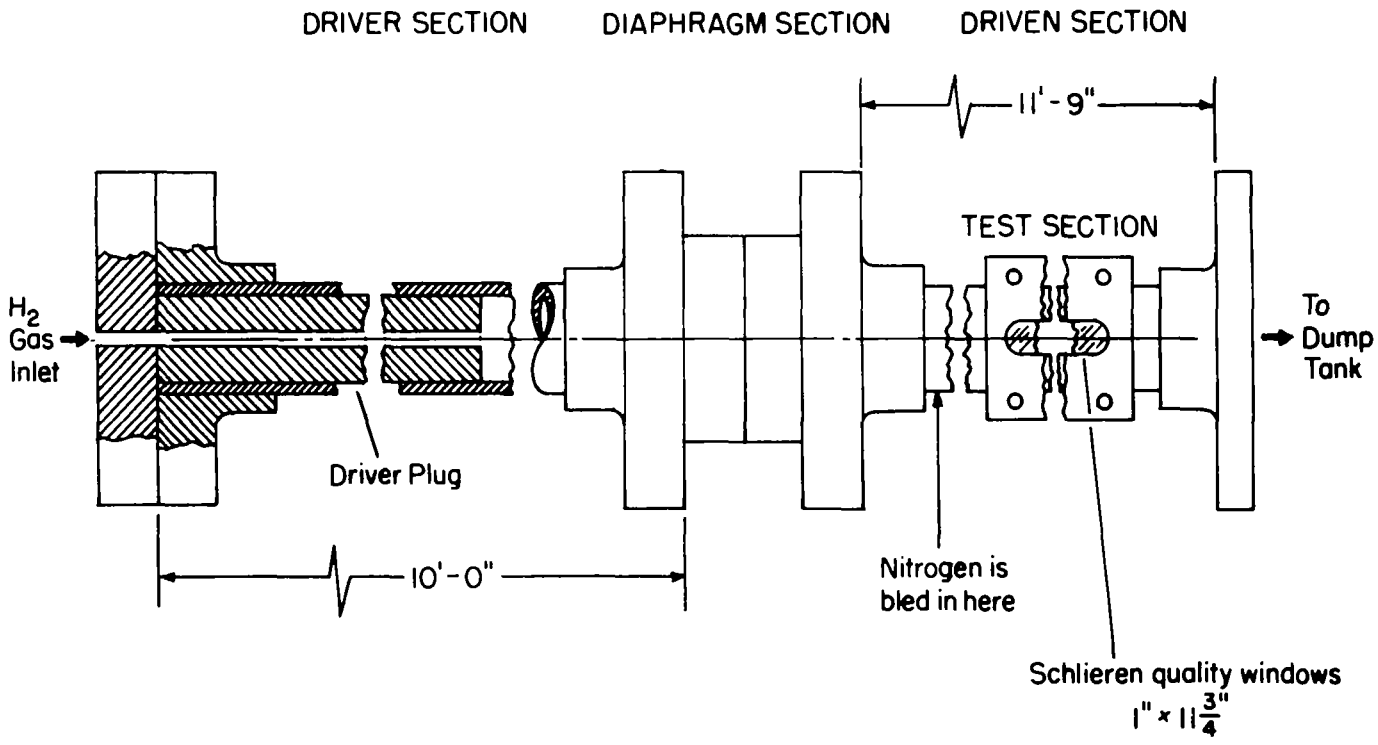

Figure 32. Shock Tube for Drop Breakup Experiments.

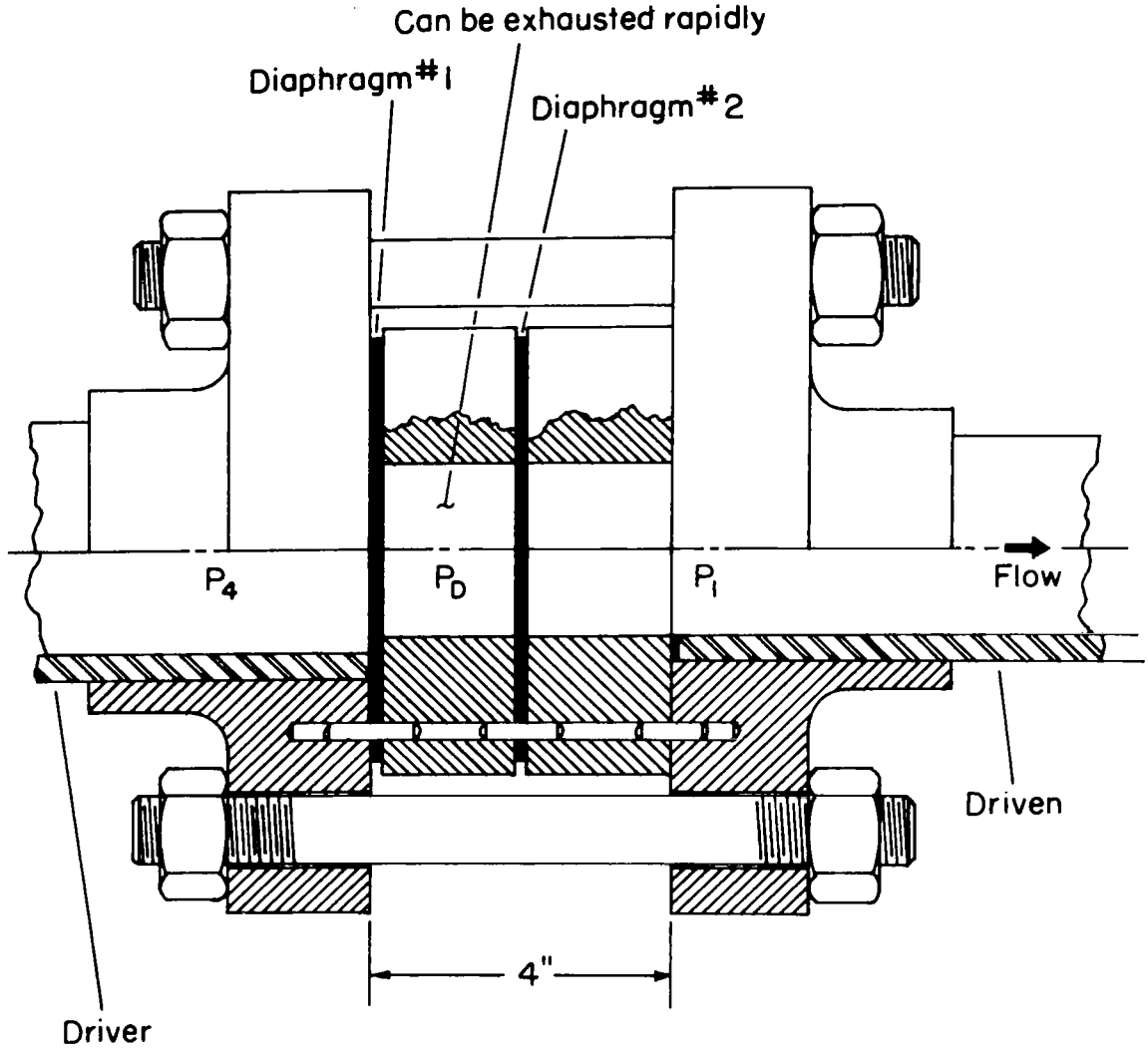

Figure 33. Double Diaphragm Section.

The driver section is fabricated from a 3 in. I. D. schedule 80 seamless stainless steel pipe 10 ft long. This length provides a 2 msec testing time at $M_s = 2$. For the higher Mach number experiments, it is expected that a testing time considerably less than 2 msec will be adequate due to shorter droplet breakup times and therefore a driver 10 ft in length is not required. For this reason the driver section is designed to accommodate end plugs which effectively reduce its length. Aside from allowing the use of a minimum quantity of the driver gas, this design minimizes the final pressure in the entire tube.

The driven section of the shock tube is a rectangular tube with internal dimensions of 1. 5 x 2. 5 in. with a 3/8 in. thick wall of seamless stainless steel 12 ft long which empties into a dump tank. The driven section and the dump tank have been designed to withstand the working pressures associated with a shock Mach number $M_s = 8$ and $p_1 = 1$ atmosphere.

The test section was made by cutting a slot in each side of the driven tube 9 ft from the diaphragm. Schlieren quality plate glass windows 11 3/4 in. long, 1 in. wide, and 1 3/16 in. thick are held in flanges which fit into the slots on either side of the tube. The windows are flush with the inside wall of the shock tube so that no flow disturbance will be created in the test section.

The passage of the wave will be sensed by two Kistler model 601A quartz transducers placed at a known distance apart. Their outputs will be used to trigger a CMC model 757B time interval meter so that measurement of the wave speed can be made.

To preclude the possibility of a hydrogen explosion, steps have been taken to avoid a hydrogen-oxygen mixture from existing anywhere in the system. Initially, nitrogen will be used as the test gas in the driven section and after each test the hydrogen-nitrogen mixture that remains will be purged from the system by bleeding nitrogen in through the end of the driver section and out through the exhaust system.

The capabilities of the shock tube are shown in Fig. 35 and 36. In Fig. 35 the Mach number of the shock wave as a function of the diaphragm pressure ratio is shown. When the test section pressure is one atmosphere, it can be seen that for commercially available hydrogen (at 2200 psi) the maximum Mach number attainable is about 5. To obtain higher Mach numbers, for the same hydrogen pressures, the driven section pressure can of course be lowered. Unfortunately this affects both the Reynolds and the Weber numbers and therefore in order to increase the range of these parameters, higher pressures in the driver section—obtainable by a pressurizing system—have to be used. The pressurizing system will be designed later.

Figure 36 shows the range in Reynolds and Weber numbers obtainable if the test section is initially at one atmosphere. For a 1 mm diameter water drop, the Weber number range is 10^4 - 7 x 10^5 and the Reynolds number range is 5 x 10^4 - 2.5 x 10^5 when air is used. These ranges are much higher than what have been used in the past and can of course be modified by a change in the drop diameter and its surface tension.

Since it will be necessary to place droplets of known size into the test section, a drop producing mechanism similar to that described in Section III will be used. Because the drops are introduced into the

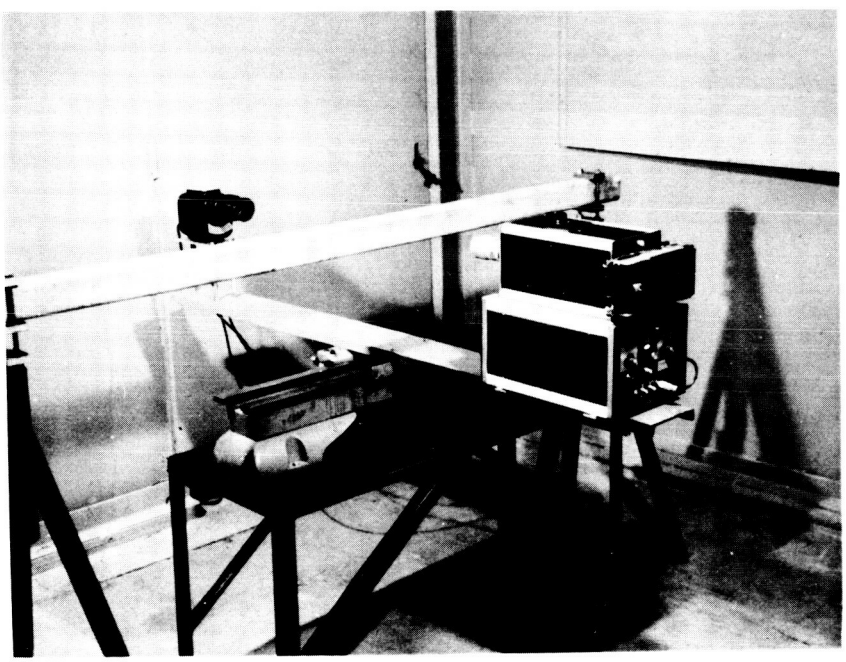

Figure 34. Photograph of the Optical Bench Mounted Under Mock-up of the Driven Section.

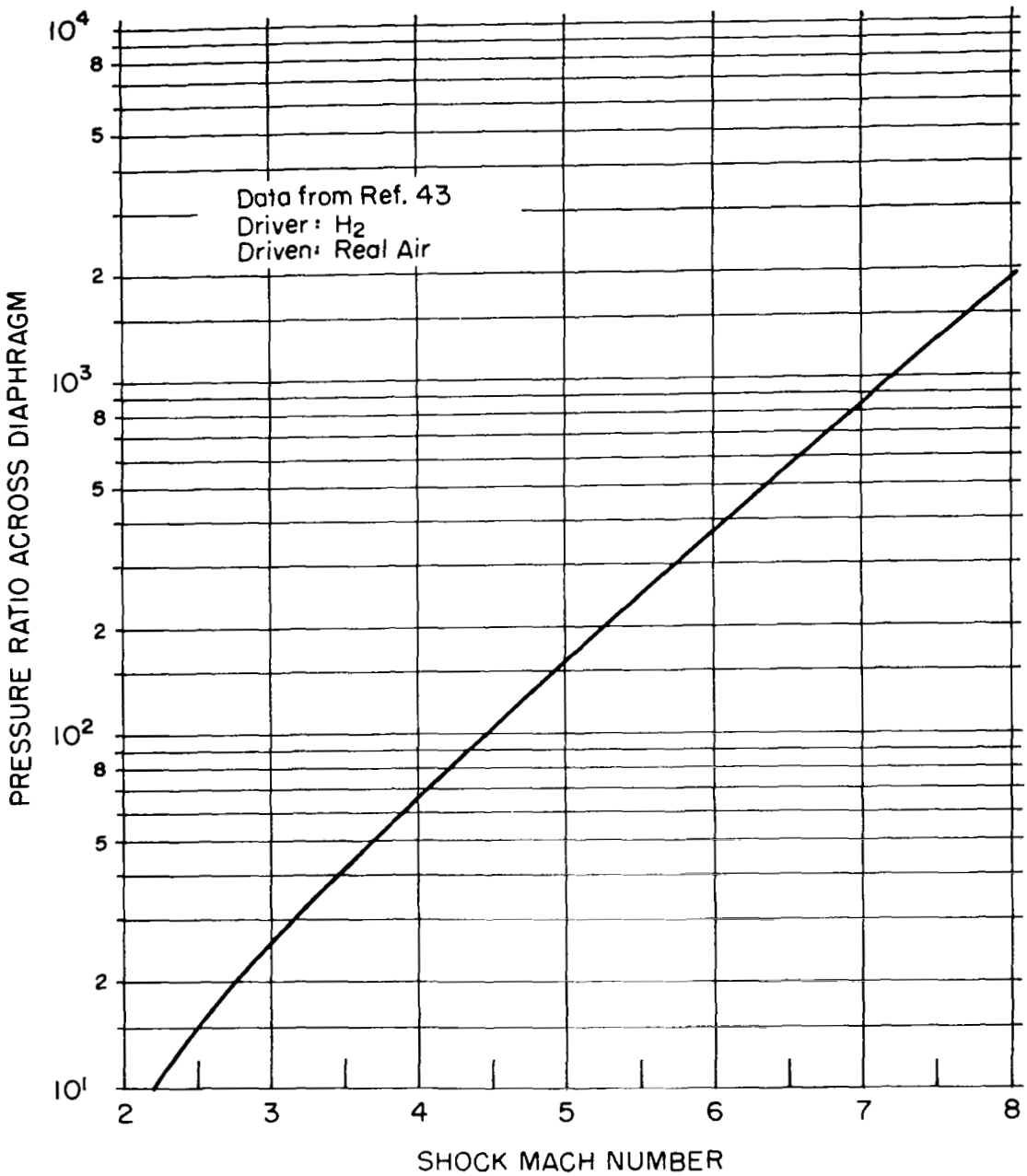

Figure 35. Relation Between Pressure Ratio Across Diaphragm and Shock Mach Number.

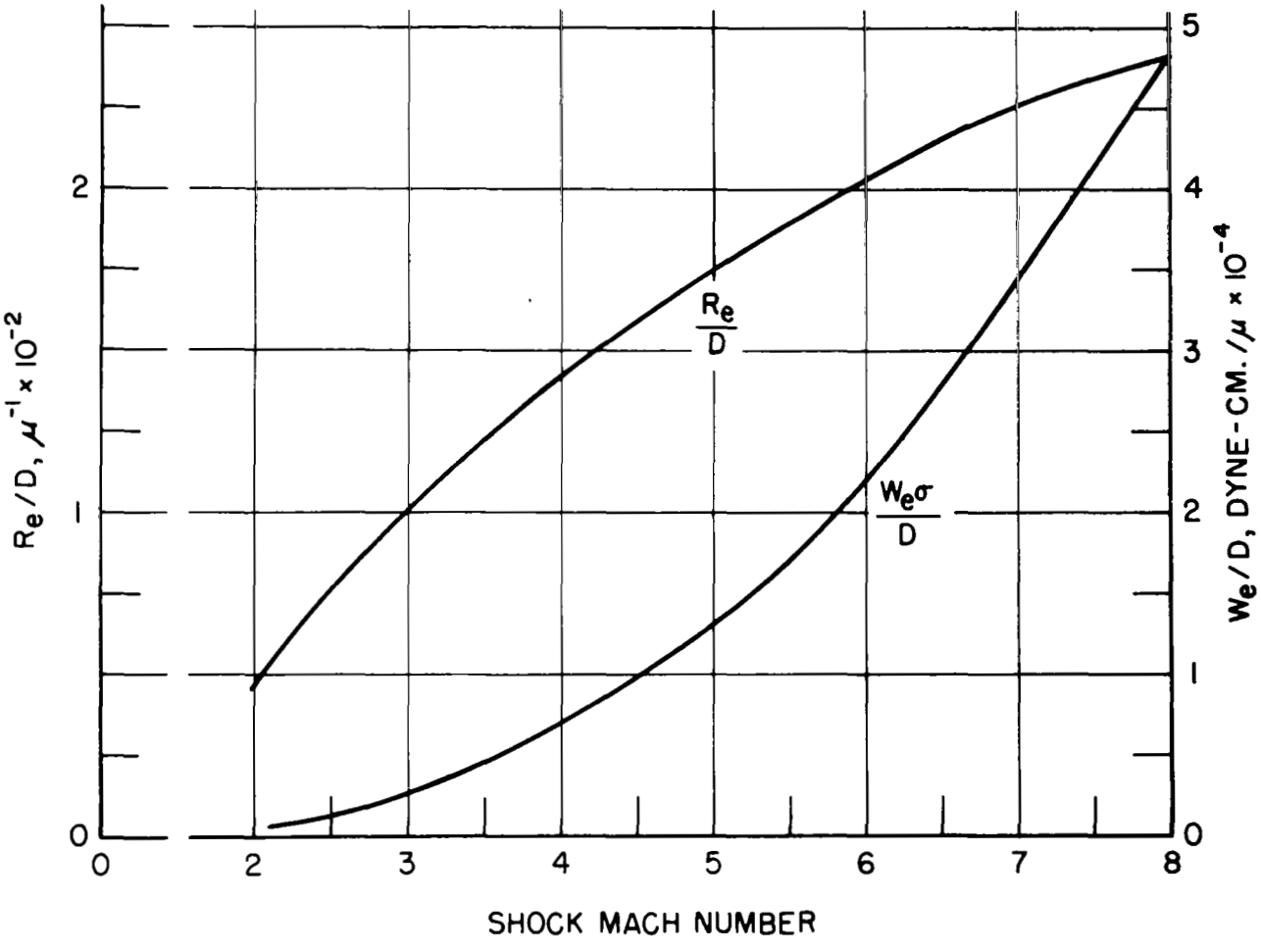

Figure 36. Weber and Reynolds Numbers Variation with Shock Mach Number in Equilibrium Air.

test section through holes in the tube walls, it is desirable that the pressure in the driven section be atmospheric. For conditions where this pressure must be reduced, the drop producing mechanism will have to be fully enclosed for the purpose of evacuation.

Since the drop breakup time behind a strong shock is of the order of microseconds, an extremely short exposure time is dictated. Nanosecond exposures will be taken using a Beckman and Whitley type 501A image converter camera in conjunction with a synchronized spark light source. The camera and spark are synchronized internally and may be delayed up to 100 microseconds after wave passage. By taking several pictures at different time intervals, a photographic time history of the drop breakup may be recorded. The image converter camera and light source are mounted on a piece of channel iron which is bolted across the saddle of a 48 in. lathe bed. Figure 34 shows the camera, source, and lathe bed mounted under a mock-up of the driven section. The saddle may be translated along the lathe bed to move the optical path as required. The camera is triggered by a transient light detector that responds to the light pulse from a dark-field schlieren system. This system senses the passage of the wave into the test section.

Only one photograph is made each time the shock tube is fired so that a time history of the breakup process will be obtained through a series of pictures made in successive runs. This diagnostic technique was also employed by Engel[39] who used it with great success in a shock tube study of water drop breakup. The entire shattering process can be pictorially recorded starting with the moment a shock wave and droplet first interact until that time at which the breakup process essentially has gone to completion. Since the wave speed and the droplet

size and trajectory can be controlled within extremely small limits, excellent test similarity in successive runs is assured.

From the experimental data one then would hope to formulate a general expression for the droplet breakup time as a function of the variables employed in the study. Such a formulation would be highly useful in defining an analytical model for the propagation of a detonation wave in a droplet-gas system as it would supply a much better estimation of the vaporization rate input to the analysis. Also, from enlargements of the photographs, it is hoped that details of the non-linear surface wave development on the droplet will become visible. Rojec[45], in a photographic study of droplet breakup at low shock Mach numbers, obtained pictures containing an amazing amount of detail. From his pictures it is not only possible to observe the rate at which the surface waves propagate from the front to the rear stagnation point but one is also able to measure their wavelength and amplitude as a function of time.

V. SUMMARY OF RESULTS

1. The theoretical jump conditions in spray detonations show that the molecular weight can have significant effects when these conditions are compared with those of the all-gaseous case counterparts.

2. It was possible to produce at least a "detonation-like" wave in a heterogeneous system of liquid DECH and gaseous oxygen. For a stoichiometric mixture the wave speed was 5300-5700 ft/sec and the peak pressure jump was ~ 30:1.

3. A self maintained detonation-like wave which propagates at lower velocity can also be produced by a transmitted shock through a tube in which the walls are wetted by the fuel. The ease with which such a wave can be produced is considered significant to the problem of rocket motor instability.

4. Means of producing monodisperse sprays adaptable to this study are discussed.

5. The design of a shock tube for the study of drop shattering—considered a basic phenomenon in spray detonation—has been completed. The purpose of this tube is to obtain experimental results under Reynolds and Weber number ranges encountered in detonations.

VI. FUTURE PLANS

1. Further experimental studies on spray detonations will be conducted. Monodisperse sprays will be used whenever possible. Emphasis will be made on non-wall wetting sprays to ascertain any difference in initiation.

2. Theoretical treatment of the wall wetted case as well as the monodisperse spray case will be attempted.

3. Improvements in producing monodisperse sprays will be made.

4. Experimental studies on drop shattering will be started with the aim of checking on the relevant parameters and reaching a unified theoretical treatment.

REFERENCES

1. Rupe, J. H. and Clayton, R. M., Jet Propulsion Laboratory, private communication.

2. Williams, F. A., "Detonations in Dilute Sprays," Progress in Astronautics and Rocketry, Academic Press, New York, 1962, Vol. 6, pp. 99-114.

3. Williams, F. A., "Progress in Spray-Combustion Analysis," Eighth International Symposium on Combustion, The Williams and Wilkins Company, Baltimore, 1962, pp. 50-69.

4. Webber, W. F., "Spray Combustion in the Presence of a Travelling Wave," Eighth International Symposium on Combustion, The Williams and Wilkins Company, Baltimore, 1962, pp. 1129-1140.

5. Cramer, F. B., "The Onset of Detonation in a Droplet Combustion Field," Ninth International Symposium on Combustion, Academic Press, New York, 1963, pp. 482-487.

6. Diethylcyclohexane, Technical Data Sheet, Monsanto Chemical Company, January 12, 1959.

7. , Evaluation of Hydrocarbons for High Temperature Jet Fuels, Part II. Fuel Evaluation and Property Correlation, Volume II. Hydrocarbon Properties, WADC TR 59-327.

8. Rabin, E., Schallenmuller, A. R., and Lawhead, R. B., Displacement and Shattering of Propellant Droplets, AFOSR TR 60-75, Rocketdyne, March 1960.

9. Chemical Engineers' Handbook, Third Edition, McGraw-Hill, 1950, p. 564.

10. Morrison, R. B., A Shock Tube Investigation of Detonative Combustion, Report UMM 97, The University of Michigan, January 1952.

11. Burgoyne, J. H. and Cohen, L., "Effect of Drop Size on Flame Propagation in Liquid Aerosols," Proc. Roy. Soc., 1954, Vol. A225, No. 1162, pp. 375-392.

12. York, J. L. and Stubbs, H. E., "Photographic Analysis of Sprays," Trans. ASME, Oct. 1952, Vol. 74, No. 7, pp. 1157-62.

13. Ingebo, R. D., "Atomization, Acceleration and Vaporization of Liquid Fuels," Sixth International Symposium on Combustion, Reinhold Publishing Corp., New York, 1957, pp. 684-7.

14. Bensen, G. M. et al., "Flourescent Technique for Determining the Cross-Sectional Drop Size Distribution of Liquid Sprays," ARS J., 1960, Vol. 30, pp. 447-454.

15. Ingebo, R. D., "Size Distribution and Velocity of Ethanol Drops in a Rocket Combustion Burning Ethanol and Liquid Oxygen," ARS J., April 1961, p. 540.

16. Dobbins, R. A., Crocco, L., and Glassman, I., "Measurement of Mean Particle Sizes of Sprays from Diffractively Scattered Light," AIAA J., August 1963, pp. 1882-6.

17. Burgoyne, J. H. and Cohen, L., "Production of Monodisperse Aerosols of Large Drops," J. Colloid Sci., 1953, 8 (3), p. 364.

18. Sinclair, D. and LaMer, V. K., "Light Scattering as a Measurement of Particle Size in Aerosols," Chem. Rev., 1949, 44, p. 245.

19. LaMer, V. K., Inn, E. C. Y., and Wilson, I. B., "The Method of Forming Detecting and Measuring the Size and Concentration of Liquid Aerosols in the Size Range 0.01-.25 microns Diameter," J. Colloid Sci., 1950, 5, pp. 471-497.

20. Vonnegut, B. and Neubaur, R., "Production of Monodisperse Liquid Particles by Electrical Atomization," J. Colloid Sci., 1952, 7 (6), p. 616.

21. Dimmock, N. A., "Production of Uniform Droplets," Nature (Engl), 1950, Vol. 166, pp. 686-687.

22. Dimmock, N. A., "The Controlled Production of Streams of Identical Droplets," Nat. Gas Tub. Est. (Engl), Memo M 115, 1961.

23. Magarvey, R. H. and Taylor, B. W., "Apparatus for the Production of Large Water Drops," The Rev. of Sci. Inst., Nov. 1956, Vol. 27, No. 11, pp. 944-47.

24. Mason, B. J., Jayaratne, P. W., and Woods, J. D., "An Improved Vibrating Capillary Device for Producing Uniform Water Droplets of 15 to 500 μm Radius," J. Sci. Inst., 1963, Vol. 40, pp. 247-49.

25. Mason, B. J. and Brownscombe, J. L., "Production of Uniform Size Drops at Controllable Frequency and Spacing from a Vibrating Capillary," J. Sci. Inst., May 1964, Vol. 41, pp. 258-259.

26. Raynor, A. C. and Haliburton, W., "Rotary Device for Producing a Stream of Uniform Drops," Rev. of Sci. Inst., 1955, Vol. 26, pp. 1124-1127.

27. Wolf, W. R., "Study of the Vibrating Reed in the Production of Small Droplets and Solid Particles of Uniform Size," Rev. of Sci. Inst., 1961, 32, No. 10, pp. 1124-29.

28. Schlichting, H., Boundary Layer Theory, McGraw Hill Co., New York, 1955, p. 16.

29. Rayleigh, J. W. S., "Instability of Jets," Proc. London Math Soc., 1878, Vol. 10, pp. 4-13.

30. Savart, F., "Memoir sur la Constitution des Veines Liquide Lancees par des Orifices Circulaires en Mince Paroi," Ann de Chimie LIII, 1933, Vol. 53, pp. 337-387.

31. Schneider, J. M. and Hendricks, C. D., "Source of Uniform-Sized Liquid Drops," Rev. of Sci. Inst., Nov. 1964, 35, pp. 1349-50.

32. Weber, C., "Zum Zerfall eines Flussigkeitsstrahles," Zt. angew. Math. und Mech., 1931, 11, pp. 136-154.

33. Crane, L., Birch, S., and McCormack, P. D., "The Effect of Mechanical Vibration on the Break-up of a Cylindrical Water Jet in Air," B. J. of App. Phys., 1964, Vol. 15, pp. 743-750.

34. Schneider, J. M., The Stability of Electrified Liquid Surfaces, Report No. CPRL-2-64, Charged Particle Research Lab., U. of Illinois, March 1964.

35. Sweet, R. G., High Frequency Oscillography with Electrostatically Deflected Ink Jets, Tech. Report No. 1722-1, Stanford Electronics Lab., Stanford U., March 1964.

36. Bredfelt, H. R., Evaluation of a Light Scattering Technique for Determining the Spray Characteristics of Impinging Liquid Jets, Tech. Report No. 648, Dept. of Aeros. and Mech. Sciences, Princeton U., March 1964.

37. Luther, F. E., "Electrostatic Atomization of No. 2 Heating Oil," Proc. API Research Conference on Distillate Fuel Combustion, Am. Petr. Inst. Div., Marketing, N. Y., 1962, p. 23.

38. Nicholls, J. A. and Cullen, R. E., The Feasibility of a Rotating Detonation Wave Rocket Motor, RPL-TDR-113, The U. of Michigan, April 1964.

39. Engel, O. G., "Fragmentation of Waterdrops in the Zone Behind an Air Shock," J. of Res., NBS, March 1958, Vol. 60, No. 3.

40. Hanson, A. R., Domich, E. G., and Adams, H. S., An Experimental Investigation of Impact and Shock Wave Breakup of Liquid Drops, Res. Report 125, U. of Minnesota, Inst. of Tech., Dept. of Aero. Eng., January 1956.

41. Hanson, A. R. and Domich, E. G., The Effect of Liquid Viscosity on the Breakup of Droplets by Air Blasts—A Shock Tube Study, Res. Report 130, U. of Minnesota, Inst. of Tech., Dept. of Aero. Eng., June 1956.

42. Morrell, G. and Povinelli, F. P., Breakup of Various Liquid Jets by Shock Waves and Applications to Resonant Combustion, NASA TN D 2423, Lewis Res. Cntr., Cleveland, Ohio, August 1964.

43. Glass, I. I. and Hall, G. J., Handbook of Supersonic Aerodynamics Section 18 on Shock Tubes, NAVORD Report 1488, December 1959, Vol. 6.

44. Byron, S., "Dissociation Studies of Oxygen," J. of Chem. Phys., June 1959, Vol. 30, No. 6.

45. Rojec, E. A., Photographic Presentation of Shear Type Droplet Breakup, Res. Report 63-39, Rocketdyne, November 1963.